University of Szeged

Faculty of Pharmacy

Institute of Pharmacodynamics and Biopharmacy

In vitro and *in vivo* evaluation of the antineoplastic potential of novel D-ring-modified estrone derivatives

Ph.D. Thesis

Sándor Bartha

Supervisor:

Dr. Renáta Minorics, Ph.D.

2026

LIST OF PUBLICATIONS RELATED TO THE SUBJECT OF THE THESIS

I. Kiss A, Jójárt R, Mernyák E, **Bartha S**, Minorics R, Zupkó I, Schneider G. Novel preparation of substituted oxazolines condensed to D-ring of estrane skeleton and characterization of their antiproliferative properties. *Steroids.* **176,** 108911 (2021).
DOI: https://doi.org/10.1016/j.steroids.2021.108911
IF: 2.76 / Q2

II. Mernyák E, **Bartha S**, Kóczán L, Jójárt R, Resch V, Paragi G, Vágvölgyi M, Hunyadi A, Bruszel B, Zupkó I, Minorics R. Microwave-assisted Phospha-Michael addition reactions in the 13α-oestrone series and *in vitro* antiproliferative properties. *J Enzyme Inhib Med Chem.* **36,** 1931-1937 (2021).
DOI: https://doi.org/10.1080/14756366.2021.1963241.
IF: 5.756 / Q2

III. **Bartha S**, Germán P, Bózsity N, Puskás LG, Börzsei R, Hetényi C, Zupkó I, Mernyák E, Minorics R. Biological and computer-aided evaluation of 3-methoxy-13α-estrone-16α-diphenylphosphine oxide as a new antiestrogenic agent. *Sci Rep.* **15,** 44295 (2025).
DOI: https://doi.org/10.1038/s41598-025-27905-x
IF: 3.9 / Q1

ADDITIONAL PUBLICATIONS

i. Ristovski (Trifunović) J, Minorics R, **Bartha S**, Janković N, Zupkó I. The evaluation of the anticancer activity of the Biginelli hybrids and pharmacokinetic profiling based on their retention parameters. *J Mol Struct*. **1254,** 132373 (2022).
DOI: https://doi.org/10.1016/j.molstruc.2022.132373.
IF: 3.8 / Q2

Table of Contents

1. Introduction

1.1. Overview of global cancer epidemiology and etiology

Cancer continues to be one of the leading causes of morbidity and mortality worldwide, being a major public health and socioeconomic challenge in the 21st century. According to the reports of Global Cancer Observatory (GLOBOCAN) of the International Agency for Research on Cancer (IARC), approximately 20 million new cancer cases and more than 9.7 million cancer-related deaths occurred in 2022 alone, with lung, female breast, colorectal, prostate, stomach and liver cancers accounting for approximately 50% of new cancer diagnoses and almost 55% of cancer-related deaths [1]. The expected growth of the cancer burden globally over the coming decades is significant, driven primarily by demographic changes such as aging populations and increasing incidence rates of various cancers. Projections indicate that the annual global cancer burden will continue to rise, with cancer incidence and prevalence estimated to increase substantially by 2050, particularly among individuals aged 65 and older [2].

The burden of cancer is not evenly distributed across the world, countries and regions with higher Human Development Index (HDI) values tend to show higher age-standardized incidence rates but lower age-standardized mortality rates for many common cancer types. This pattern arises from the longer life expectancy of the higher-HDI regions, which increases the chance of developing cancer, more widespread diagnostic services, screening, and generally better access to effective curative and supportive treatments, leading to improved survival. Conversely, low- and medium-HDI countries often have lower recorded incidence but proportionally higher mortality because cancers are more frequently diagnosed at advanced stages and health-system constraints limit timely, effective treatment [1].

The etiology of cancer is multifactorial, involving both intrinsic genetic susceptibilities and extrinsic environmental exposures. Well-established risk factors include tobacco use, alcohol consumption, unhealthy diet, lack of physical activity, and chronic infections such as human papillomavirus (HPV), hepatitis B and C viruses, and *Helicobacter pylori* [3,4].

Chronic infections also play a significant role in cancer development, with HPV linked to cervical and head and neck squamous cell carcinomas, hepatitis B and C viruses to hepatocellular carcinoma, and *H. pylori* to gastric cancer [5]. Genetic predisposition, including germline mutations in tumor suppressor genes such as *BRCA1*, *BRCA2*, and *TP53*, significantly elevates lifetime risk for specific cancers, particularly breast and gynecological malignancies [6]. For example, *BRCA1* and *BRCA2* mutation carriers face a lifetime breast cancer risk of

approximately 65% and 45%, respectively [7]. Germline mutations in TP53, as seen in Li-Fraumeni syndrome, confer an 80–90% lifetime risk of breast cancer, often with early onset and multi-organ involvement [8].

Although primary tumors are often treated effectively with surgery or localized therapy, metastatic disease remains the predominant cause of cancer-related mortality, contributing to approximately 90% of deaths. [9]. Metastasis involves the dissemination of cancer cells from the primary tumor to distant organs, where they establish secondary tumors that are difficult to eradicate and often show resistance to therapy [10]. These secondary lesions compromise organ function and promote systemic complications, which together drive poor survival outcomes [11]. Population studies indicate that most cancer fatalities are attributable to metastatic disease, highlighting its central role in cancer lethality and the urgent need for therapeutic strategies targeting metastatic progression.

1.2. Breast cancer epidemiology, etiology and therapeutic options

Breast cancer, with approximately 2.3 million new cases, and more than 665,000 deaths reported only in 2022, remains the most frequently diagnosed type of cancer and the leading cause of cancer-related death among women worldwide [1].

This type of cancer arises through a multistep process that includes genetic mutations, hormonal imbalances, and immune evasion mechanisms. The transformation begins with ductal hyperplasia, advances through carcinoma *in situ*, and may progress to invasive disease through interactions with the tumor microenvironment and evasion of immune surveillance [12]. Pathologically, breast cancer is divided into invasive and lobular carcinoma, with further immunohistochemical subclassification into hormone receptor-positive (HR^+), HER2-positive ($HER2^+$), and triple-negative breast cancer (TNBC). More detailed molecular profiling, such as PAM50 and single-cell transcriptomics, has refined breast cancer subtypes into luminal A, luminal B, HER2-enriched, and basal-like, each with unique clinical implications for treatment and prognosis [13].

A central feature of HR^+ breast cancer, particularly estrogen receptor-positive (ER^+) tumors, is its dependence on estrogen signaling for growth. ER-positivity, present in about 70-80% of breast cancers, is typically detected by immunohistochemistry. ER^+ tumors tend to grow slower and carry a better prognosis than ER-negative types [14,15]. Importantly, ER-positivity strongly predicts responsiveness to endocrine (hormonal) therapies, making it a critical biomarker for treatment planning [16].

Endocrine therapy remains the mainstay for managing ER^+ breast cancer, both in the adjuvant and metastatic settings. In premenopausal women, tamoxifen, a selective estrogen receptor modulator (SERM), is the primary agent of choice. Tamoxifen binds competitively to the estrogen receptor, blocking estrogen-mediated gene transcription. In postmenopausal women, aromatase inhibitors (AIs), such as anastrozole, letrozole, and exemestane, are preferred. These agents inhibit the aromatase enzyme, which catalyzes the peripheral conversion of androgens to estrogens, effectively lowering circulating estrogen levels [17].

For patients at higher risk of recurrence, extended endocrine therapy up to 10 years is now standard, as longer durations have been shown to reduce recurrence risk and improve survival [18]. However, resistance to endocrine therapy, either intrinsic or acquired, is a major barrier to durable responses in the metastatic setting.

To address endocrine resistance, several classes of targeted agents have been developed and approved. One of the most impactful innovations has been the introduction of cyclin-dependent kinases 4 and 6 (CDK4/6) inhibitors, such as palbociclib, ribociclib, and abemaciclib [19]. These agents inhibit CDK4/6, which regulate cell cycle progression. When combined with endocrine therapy, CDK4/6 inhibitors have demonstrated significant improvements in progression-free survival and, in some studies, overall survival in metastatic ER^+ breast cancer [20]. Notably, abemaciclib has also shown benefit in the adjuvant setting for high-risk early-stage ER^+ breast cancer [21].

Another important therapeutic target in ER^+ breast cancer is the PI3K/AKT/mTOR pathway, which is frequently activated by oncogenic *PIK3CA* mutations. Activating mutations in *PIK3CA* occur in approximately 40% of $ER^+/HER2^-$ breast cancers and are associated with endocrine therapy resistance [22]. Targeting this pathway has shown clear clinical benefit: the PI3Kα-selective inhibitor alpelisib, in combination with fulvestrant, significantly improved progression-free survival in patients with *PIK3CA*-mutant advanced disease, as demonstrated in the phase III SOLAR-1 trial [23]. Similarly, inhibition of downstream mTOR signaling with everolimus combined with exemestane prolonged progression-free survival in patients previously treated with nonsteroidal aromatase inhibitors, as shown in the BOLERO-2 study [21].

In further efforts to overcome recurrent ER^+ breast cancer, fulvestrant, a pure antiestrogen and one of the earliest selective estrogen receptor degraders (SERDs), represented a significant milestone in this area. Unlike conventional SERMs, fulvestrant directly binds to the ER and facilitates its degradation, resulting in more thorough suppression of estrogen signaling [25]. Approved in 2002, fulvestrant has become a standard therapy for

postmenopausal women with advanced ER^+ breast cancer, especially in cases where other endocrine treatments have failed [23]. However, fulvestrant suffers from poor bioavailability and requires monthly intramuscular injections, which limit dosing flexibility and patient convenience. These shortcomings have driven the development of novel SERDs with improved oral availability and superior pharmacological profiles [27].

In recent years, efforts have increasingly focused on developing next-generation SERDs with enhanced effectiveness and improved pharmacokinetic properties. Ongoing research continues to expand the range of SERDs, including both steroidal and non-steroidal compounds. Elacestrant, the first oral SERD approved for use in patients with ESR1 mutations, showed superiority over standard endocrine therapy in the phase III EMERALD trial, and received FDA approval for this indication in 2023 [28,29].

1.3. Anticancer steroids

Steroids represent a diverse group of biologically active compounds, composed of four fused rings: three cyclohexane rings (A-, B-, and C-rings) and one cyclopentane ring (D-ring). This core structure serves as a versatile scaffold, and subtle modifications in functional groups, oxidation states, or stereochemistry result in a remarkable diversity of steroid molecules, encompassing hormones such as estrogens, androgens, glucocorticoids, and mineralocorticoids. Due to their high lipophilicity, steroids easily penetrate cell membranes and interact with various intracellular targets, including enzymes and receptors such as aromatase, sulfatase, 5α-reductase, hydroxysteroid dehydrogenase, and steroidal hormone receptors [30–35]. Moreover, most steroidal compounds are generally associated with favorable pharmacological properties, including low cytotoxicity and high bioavailability [36].

The connection between steroids and cancer has been studied extensively. Early observations showed that castration in animals and humans impacts the development and function of organs like the prostate and mammary glands [37]. In the 1940s, Charles B. Huggins was the first to establish the link between prostate cancer progression and sex steroids. He demonstrated that androgen deprivation, achieved through castration, could serve as an effective treatment for prostate cancer and metastatic castration-sensitive prostate cancer [38]. Advancements in computational (*in silico*) technologies have further enhanced our understanding of how steroids influence cancer cells [39,40]. Sex hormones such as testosterone and 17β-estradiol (E2) promote cell proliferation and differentiation and regulate metabolism by binding to androgen and estrogen receptors in the cytoplasm. Upon receptor

binding, these hormone-receptor complexes dimerize and move into the nucleus, where they provoke conformational changes at certain DNA regions, known as hormone responsive elements (HREs) [41,42]. This interaction induces local conformational changes in chromatin and enables the hormone-receptor complexes to function as transcriptional regulators, activating or repressing genes involved in cell growth [43–45]. This regulatory mechanism is especially significant in hormone-dependent cancers, which originate in reproductive and mammary tissues, including ovarian, breast, prostate, and endometrial cancers [46]. In clinical practice, several antineoplastic agents with a steroidal core structure are in use; these compounds either inhibit endogenous hormone biosynthesis (*e.g.*, exemestane) or interfere with hormone-receptor interactions (*e.g.*, fulvestrant, cyproterone acetate) [25,47,48].

Another pioneering observation made by Stenkvist and colleagues showed that women receiving cardiac glycosides for heart conditions exhibited notably smaller, more uniform breast tumors, suggesting a potential anticancer effect of these steroid-related compounds [49]. Subsequent studies demonstrated that cardiac glycosides inhibit tumor cell proliferation and induce apoptosis *via* pathways including inhibition of Na^+/K^+-ATPase, perturbation of intracellular ion homeostasis, caspase activation, and modulation of signaling networks like NF-κB and death receptor pathways [50,51].

Although E2 has traditionally been regarded as a potent mitogenic hormone, some estrogens display additional biological properties, such as neuroprotective, antiangiogenic, and anticancer activities. In the early 1990s, an endogenous metabolite of E2, 2-methoxyestradiol (2-ME2) was identified as an inhibitor of MCF-7 breast cancer cell proliferation. Importantly, 2-ME2 represented the first estrane-based antiproliferative compound demonstrated to act independently of estrogen receptor subtype binding [52,53].

Given their direct involvement in cancer development, researchers are actively exploring new steroidal compounds, particularly those structurally related to sex hormones with potential growth-inhibitory properties. Both natural and synthetic steroid derivatives have been isolated and tested, and efforts continue to chemically modify known steroid structures to enhance their antitumor activity [54–56].

Concerning the biological effects of estrogen-related compounds, our research group (Zupkó and colleagues) has been investigating the *in vitro* antiproliferative and antimetastatic potential of this particular group of molecules for more than a decade [57]. In this study, two sets of estrone-based compounds were employed to assess their antineoplastic potential. Structural modifications, such as introducing heterocycles, altering the steroidal side chains, or incorporating heteroatoms within the steroid framework, are known to modulate their

biological properties [58]. Numerous studies have explored and characterized heteroatom-containing steroids, many of which exhibit notable cytotoxic effects against various cancer cell lines [59]. Considering the promising biological relevance of heterocyclic steroids and the established antiproliferative activity of steroidal derivatives bearing oxazoline or dihydrooxazine rings at different positions on the sterane scaffold, these compounds emerge as intriguing candidates for further exploration of their oncopharmacological potential [60,61]. In this context, we focused on the investigation of the *in vitro* growth-inhibitory effects of aryl-substituted oxazolines fused to the estrane D-ring at the sterically accessible 16α and 17α positions.

Although these compound may exert desirable antineoplastic effects, the basic structure of these compounds contains a methyl group in the 13β position, identical to the structure of E2, which means they may even have unfavorable hormonal effects. A strategy to address this problem is to chemically modify the steroid core of natural estrogens, thereby reducing unwanted estrogenic activity. Structural studies have shown that inverting the configuration of estrone at C-13 alters the conformation, and as a result, 13α-estrone analogs lack estrogenic properties [62,63]. Moreover, several organophosphorus derivatives have been reported to exhibit notable antiproliferative effects against diverse cancer types [64]. To harness the advantages of both structural frameworks, we also explored the biological evaluation of organophosphorus derivatives of 3-methyl and 3-benzyl ethers of the core-modified 16-methylene-13α-estrone.

2. Aims and Objectives

The primary aim of this study was to determine the antineoplastic potential of several D-ring-modified estrone 16α,17α-oxazoline and 16-methylene-13α-estrone derivatives. Initial screening of the test compounds was conducted through an *in vitro* viability assay using a panel of human adherent cell lines of female breast, gynecological, and oropharyngeal origin. Further testing of the most prominent compound included several additional *in vitro* and *in vivo* methodologies to gain insight into its antiproliferative and antimetastatic properties, as well as its mechanism of action.

Accordingly, detailed objectives of the experiments are clarified as follows:

- To assess the antiproliferative potential of nine D-ring-substituted estrone 16α,17α-oxazoline derivatives against a panel of human adherent gynecological and female breast cancer cell lines by means of standard MTT assay. Furthermore, the assessment of the half maximal inhibitory concentration (IC_{50}) values of the most potent test compounds.
- To determine the growth-inhibitory potential of fourteen 16-methylene-13α-estrone derivatives against a panel of human adherent gynecological cancer cell lines by means of standard MTT assay. Furthermore, the assessment of the IC_{50} values of the most potent test compounds.
- To evaluate the estrogenic activity of the most effective test compound *in vitro* using a luciferase reporter gene assay in a commercially available, stably transfected T47D cell line.
- To assess estrogenic activity *in vivo* and to gain insight into the hormonal properties of the test compound using a uterotrophic assay.
- To investigate the cell cycle arrest potential of the test compound using propidium iodide-based cell cycle analysis.
- To evaluate the antimetastatic properties of the most potent test compound using wound healing and Boyden chamber assays.

3. Materials and Methods

3.1. Chemical structures of novel D-ring modified estrone derivatives

The tested estrone 16α,17α oxazoline derivatives (Fig. 1) and organophosphorus 16-methylene-13α-estrone derivatives (Fig. 2) were synthesized by Kiss et al. and Mernyák et al., respectively, as described previously [65,66]. For all *in vitro* experiments, 10 mM stock solutions of the test compounds were prepared with dimethyl sulfoxide (DMSO).

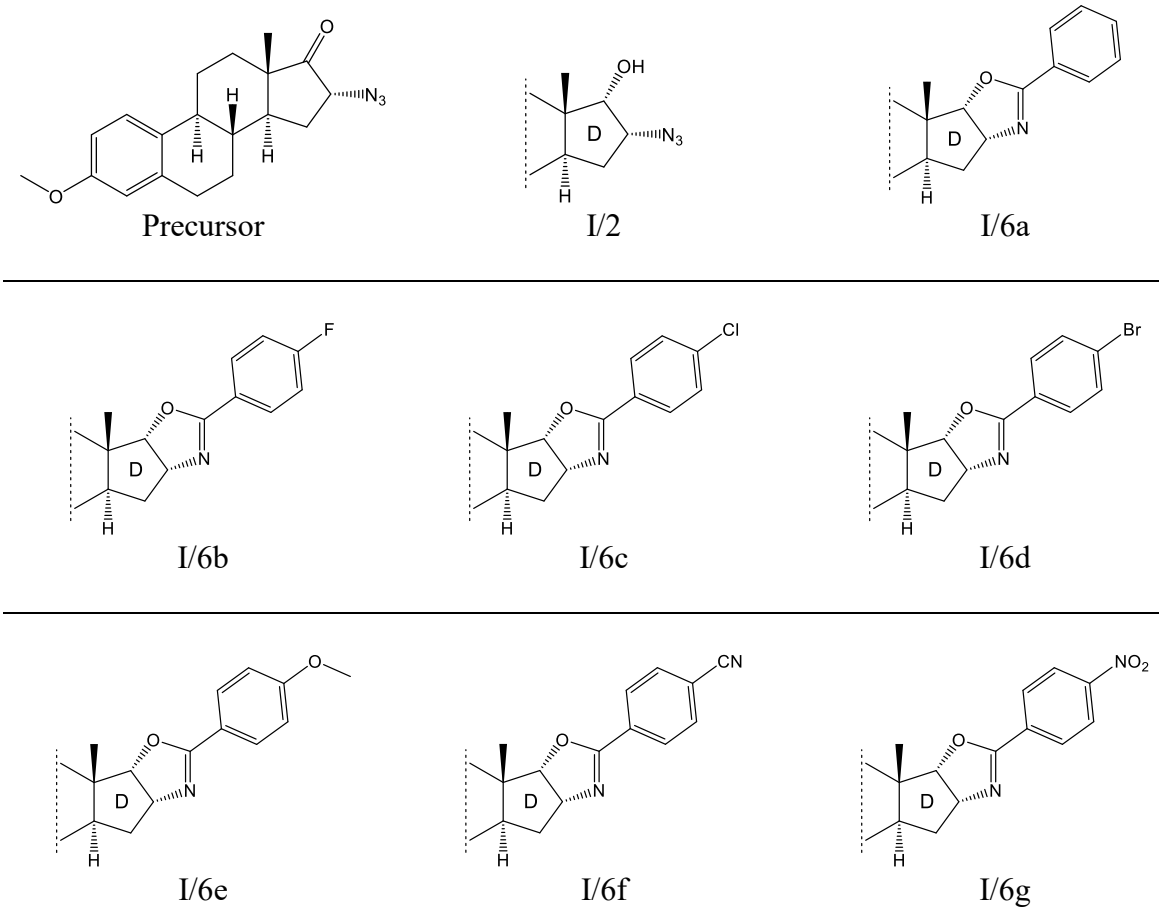

Figure 1: Chemical structures of the tested estrone 16α,17α-oxazoline derivatives

Precursors	C-16	
	α	β
	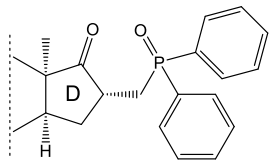 II/9 (EDPO)	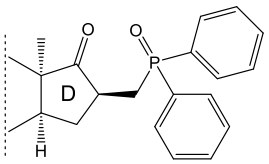 II/10
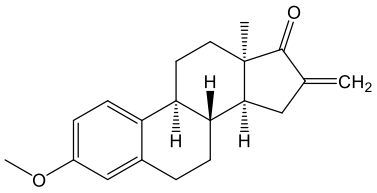 II/4	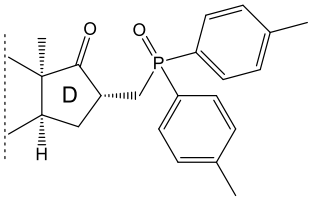 II/13	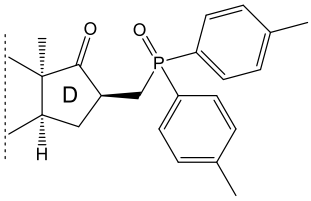 II/14
	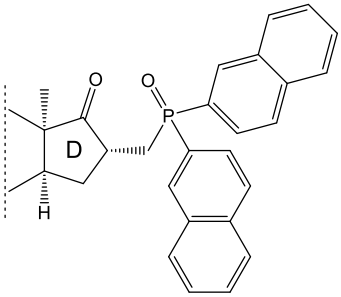 II/17	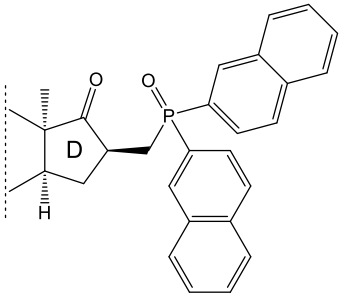 II/18
	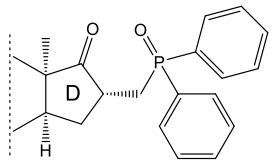 II/11	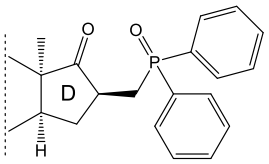 II/12
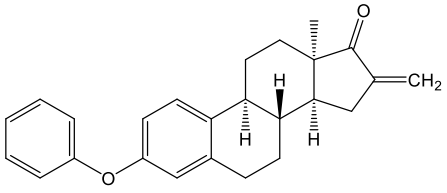 II/5	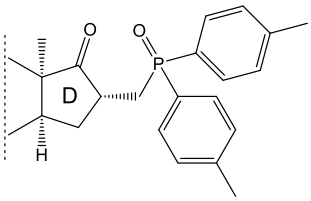 II/15	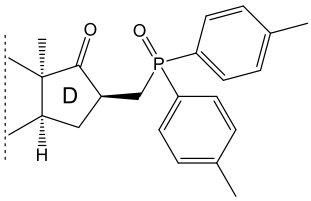 II/16
	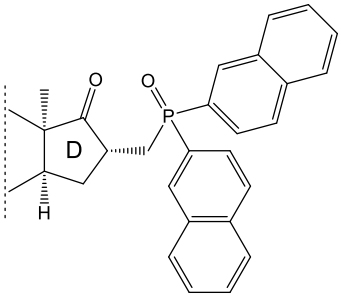 II/19	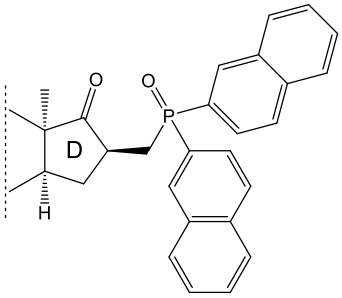 II/20

Figure 2: Chemical structures of the tested 16-methylene-13α-estrone derivatives

3.2. Cell cultures

Human adherent carcinoma cell lines (HeLa, A2780, T47D, MCF-7, and MDA-MB-231), and the non-cancerous, immortalized mouse embryonal fibroblast cell line (NIH/3T3) were purchased from ECACC (European Collection of Authenticated Cell Cultures, Salisbury, UK). Additional adherent carcinoma cell lines of human origin (SiHa, C33A) and the T47D-KBluc cell lines were obtained from ATCC (American Type Culture Collection, Manassas, VA, USA). Moreover, the oropharyngeal cancer cell lines (UPCI-SCC-131 and UPCI-SCC-154) were acquired from DSMZ (German Collection of Microorganisms and Cell Cultures GmbH, Braunschweig, Germany). The key characteristics of the cell lines used in this study are summarized in Table 1.

Cell line	Characteristics
HeLa	HPV 18-positive human cervical adenocarcinoma cell line. Highly proliferative, p53 functionally inactivated by HPV E6
SiHa	HPV 16-positive human cervical squamous cell carcinoma, with low viral copy number. Relatively lower proliferative capacity than HeLa.
C33A	HPV-negative human cervical carcinoma cell line. Carries mutant p53, allowing assessment of drug effects independent of HPV oncogene activity.
A2780	Human ovarian carcinoma cell line. Frequently used to study anticancer and hormone-related effects in gynecological malignancies.
MCF-7	Human breast adenocarcinoma, ER- and PR-positive, HER2-negative. A classical model for studying estrogen-dependent tumor growth and antiestrogenic compounds.
T47D	Human breast ductal carcinoma cell line, ER- and PR-positive, HER2-negative, expressing mutant p53. Suitable for evaluating hormone-dependent anticancer mechanisms.
MDA-MB-231	Human triple-negative breast cancer cell line (ER-, PR-, HER2-). Highly invasive and hormone-independent, serving as a contrast to ER-positive breast cancer models
UPCI-SCC-131	HPV-negative human head and neck squamous cell carcinoma cell line.
UPCI-SCC-154	HPV 16-positive human head and neck squamous cell carcinoma. Enables comparison of drug responses between HPV-positive and HPV-negative squamous cell carcinomas.
NIH/3T3	Immortalized mouse embryonic fibroblast cell line, non-tumorigenic. Commonly used as a normal control to assess compound selectivity and cytotoxicity.
T47D-KBluc	ER-positive T47D breast cancer cells stably expressing a luciferase reporter. Enables functional assessment of estrogen receptor signaling and estrogen-modulating effects of test compounds

Table 1: Characterization of the cell lines used in this study.

Cells were cultured and maintained in a Eagle's minimum essential medium (EMEM; Capricorn Scientific GmbH, Ebsdorfergrund, Germany) supplemented with 10% fetal bovine serum (FBS; Capricorn Scientific GmbH, Ebsdorfergrund, Germany), 1% non-essential amino acids, 1% L-glutamine and 1% antibiotic-antimycotic mixture. Moreover, the T47D-KBluc cell line, used in the antiestrogenic assay, was cultured in phenol red-free RPMI (Thermo Fisher Scientific Inc., Waltham, MA, USA) medium supplemented with 10% FBS, 1% non-essential amino acids, 1% L-glutamine, and 1% antibiotic-antimycotic mixture. All cell lines were maintained at 37°C in humidified atmospheric air containing 5% CO_2. All media and reagents, unless otherwise indicated, were purchased from Merck Ltd. (Budapest, Hungary).

3.3. Antiproliferative assay

The antiproliferative activity of the investigated compounds was assessed on a panel of human gynecological, female breast, and oropharyngeal cancer cell lines. Tumor selectivity was examined using the immortalized mouse fibroblast cell line NIH/3T3. Cells were seeded into 96-well plates at a density of 5,000 cells/well, with the exception of C33A cells, which were seeded at 10,000 cells/well. After 24 h, the medium was replaced with 200 µL of fresh medium containing the test compounds at concentrations of 10 or 30 µM. Cells were then incubated for 72 h at 37 °C in a humidified atmosphere with 5% CO_2. Cell viability was determined using the MTT assay by adding 20 µL of a 5 mg/mL 3-(4,5-dimethylthiazol-2-yl)-2,5- diphenyltetrazolium bromide (MTT) solution. Following a 4 h incubation, during which viable cells reduced MTT to insoluble formazan crystals, the medium was carefully removed, and the crystals were solubilized in 100 µL of DMSO with shaking at 37 °C for 60 min. Absorbance was measured at 545 nm using a SPECTROStar Nano microplate reader (BMG Labtech GmbH, Ortenberg, Germany), with untreated cells serving as the negative control. For compounds exhibiting significant activity (≥50% growth inhibition at 10 or 30 µM), the assay was repeated using a concentration range of 0.1–30 µM, and IC_{50} values were determined from sigmoidal concentration-response curves fitted using GraphPad Prism 5.01 (GraphPad Software, San Diego, CA, USA). All experiments were performed independently in duplicate, with at least five parallels per condition. Stock solutions (10 mM) were prepared in DMSO, and the final DMSO concentration did not exceed 0.3%, a level that had no significant effect on cell proliferation. Cisplatin (Ebewe Pharma GmbH, Unterach, Austria) was used as a reference compound.

3.4. Luciferase reporter gene assay

The *in vitro* antiestrogenic potential of the test compound EDPO and its 3-benzyloxy counterpart (II/11, 3-BEDPO) were evaluated using the T47D-KBluc cell line, an ERα^{+} breast cancer model that is stably transfected with an ERE-luciferase reporter gene cassette (Wilson 2004). Cells were seeded into 96-well plates at a density of 50,000 cells per well. After a 72-hour incubation period, the growth medium was replaced with phenol red-free RPMI supplemented with 10% charcoal-stripped FBS to eliminate residual estrogenic activity. This medium replacement was repeated daily for four additional days to ensure intracellular estrogen depletion.

On the ninth day, cells were exposed to 3.5×10^{-11} M E2 in combination with either fulvestrant (ranging from 1×10^{-12} to 5×10^{-8} M) or the test compounds (ranging from 4×10^{-7} to 6×10^{-5} M). Following 24 hours of treatment, the medium was removed, and ONE-Glo™ firefly luciferase reagent (Promega Corp., Madison, WI, USA) was added in accordance with the manufacturer's protocol. After a 5-minute incubation, luminescence was measured using a FLUOstar OPTIMA luminometer (BMG Labtech GmbH, Ortenberg, Germany). All concentrations were tested in triplicate and independently repeated three times. The resulting Relative Luminescence Units (RLU) were normalized to percentage values, and sigmoidal concentration-response curves were generated using GraphPad Prism 9.5.1.

3.5. *In vivo* uterotrophic assay

Following the results obtained from the *in vitro* luminometric assay, we sought to assess the antiestrogenic activity of the test compound *in vivo*. The uterotrophic assay was conducted in accordance with OECD Test Guideline No. 440 (OECD 2007). Female immature Sprague-Dawley rats (Animalab Ltd., Vác, Hungary), 21 days old and weighing between 35–47 g, were housed under controlled environmental conditions with a 12-hour light–dark cycle and had free access to tap water and a standard pellet diet (INNOVO Ltd., Gödöllő, Hungary).

Animals were randomly assigned to five experimental groups, each consisting of 6–7 rats: (1) vehicle control (vegetable oil), (2) E2 group (0.1 μg/g E2), (3) E2 + FULV (0.1 μg/g E2 + 0.3 μg/g fulvestrant), (4) E2 + EDPO (60) (0.1 μg/g E2 + 60 μg/g EDPO), and (5) E2 + EDPO (600) (0.1 μg/g E2 + 600 μg/g EDPO). Dose selection was based on previously reported ED_{50} values for E2 and our own *in vitro* antiestrogenic assay data [67]. All compounds were dissolved or suspended in vegetable oil.

Treatments were administered once daily for three consecutive days *via* subcutaneous injection, with dosages adjusted according to individual body weights. On the fourth day, animals were euthanized under deep anesthesia (2.5% isoflurane; AErane liquid for inhalation, Baxter Hungary Ltd., Budapest, Hungary), and uterine tissues were carefully excised. Wet uterine weights were recorded, and the results were compared to those of the positive control group. The experiment study was approved by the National Food Chain Safety Office (permit number: IV./397/2023).

3.6. Cell cycle analysis

To investigate the potential mechanism of action of EDPO, cell cycle distribution was analyzed in the ERα$^+$ breast cancer cell line T47D [68]. Cells were seeded into 24-well plates at a density of 2.5×10^5 cells per well and allowed to adhere overnight. Subsequently, they were treated with EMEM containing increasing concentrations of EDPO (1.75, 3.5, and 7 μM) or fulvestrant (5 μM) for 12, 24, 48, and 72 hours. The selected concentrations were determined based on the previously established IC_{50} value of EDPO and published data [66,69].

After treatment, cells were collected and centrifuged at 1500 RPM for 10 minutes at room temperature. The supernatant was discarded, and the resulting cell pellets were fixed in cold 70% ethanol. Fixed samples were centrifuged again, resuspended, and stained with a propidium iodide (PI) solution containing 10 μg/mL PI, 10 μg/mL RNase A, and 0.1% sodium citrate for 30 minutes in the dark at room temperature. DNA content was then quantified using a CytoFLEX Flow Cytometer equipped with CytExpert software (Beckman Coulter, Inc., Indianapolis, IN, USA), acquiring 20,000 events per sample.

Data were analyzed using ModFit LT 3.3.11 (Verity Software House, Topsham, ME, USA) and GraphPad Prism 5.01. Untreated cells served as controls. The sub-G1 cell population was identified as apoptotic cells. Each experiment was performed twice, with four parallel replicates per condition.

3.7. Cell migration (wound healing) assay

The antimigratory activity of the test compound was evaluated using a wound healing assay with specialized two-chamber inserts (ibidi GmbH, Gräfelfing, Germany) [70]. UPCI-SCC-131 and T47D cells were seeded into both chambers at a density of 35,000 cells per chamber and incubated overnight under standard culture conditions to allow proper cell attachment to the plate surface. After incubation, the inserts were carefully removed, and wells

were rinsed twice with 0.5 mL of phosphate-buffered saline (PBS) to eliminate unattached cells and debris.

Cells were then treated with fresh medium containing 2% FBS and sub-antiproliferative concentrations of the test compound (half of the IC_{50} and the IC_{50} values (2.5 and 5 μM for UPCI-SCC-131; 3.5 and 7 μM for T47D cells [66]) and incubated for an additional 24 or 48 hours. Cell migration into the wound area was monitored using a phase-contrast inverted microscope (Nikon Eclipse TS100, Nikon Instruments Europe, Amstelveen, The Netherlands). Representative images were captured for each condition using a CCD camera (QImaging MicroPublisher Color RTV5.0, Teledyne Photometrics, Tucson, AZ, USA) to evaluate the degree of wound closure.

The percentage of cell migration was quantified at 0, 24, and 48 hours by measuring the remaining cell-free area and comparing these values to untreated controls at the corresponding time points using ImageJ software (National Institutes of Health, Bethesda, MD, USA). All migration assays were performed twice, each with four parallel replicates per treatment.

3.8. Transwell invasion (Boyden chamber) assay

To assess the effect of the test compound on the invasive potential of T47D cells, a Boyden chamber invasion assay was performed. Specialized inserts equipped with a thin PET membrane coated with a Matrigel basement matrix (BioCoat® Matrigel® Invasion Chambers with 8.0 μm PET Membrane, Corning Inc., Corning, NY, USA) were used for this purpose. Prior to seeding, the chambers were rehydrated with serum-free EMEM for 2 hours at 37°C.

T47D cells were suspended in serum-free EMEM containing the test compound at sub-antiproliferative concentrations (half of the IC_{50} and the IC_{50} values (3.5 and 7 μM, respectively [44]) and seeded into the upper chamber at a density of 2.2×10^5 cells per insert. The lower chambers were filled with EMEM supplemented with 10% FBS, serving as a chemoattractant. Untreated cells served as negative controls. Following a 48-hour incubation, the medium was removed and non-invading cells were gently wiped from the inserts using cotton swabs.

Cells that had migrated through and adhered to the lower membrane surface were washed twice with PBS, fixed in ice-cold 96% ethanol, and stained with 1% crystal violet for 30 minutes in the dark. After staining, images of the entire membrane were captured using a microscope equipped with a CCD camera. Quantitative analysis was performed using ImageJ software (National Institutes of Health, Bethesda, MD, USA), where the total invaded cell area

was measured and expressed as a percentage relative to the control group. Each experiment was conducted twice, with duplicate samples for every treatment condition.

3.9. Statistical analysis

Statistical evaluation of the results was performed by one-way analysis of variance (ANOVA) followed by Newman-Keuls Multiple Comparison Test using the GraphPad Prism 5.01 or 9.5.1. Data were expressed as mean ± standard error of the mean (SEM) or mean ± standard deviation (SD).

4. Results

4.1. Antiproliferative assay

As previously described, two sets of D-ring modified estrone derivatives were included in this study. Initial screening of the test compounds was performed using standard MTT assay. As a first step, all compounds were applied in 10 μM and 30 μM concentration to assess their growth-inhibitory potential. Furthermore, IC_{50} values were determined only for compounds that inhibited cell growth by at least 75%.

4.1.1. Estrone 16α,17α-oxazoline derivatives

The growth-inhibitory effects of newly synthesized D-ring-modified estrogen analogues were evaluated using a panel of human gynecological cancer cell lines, including cervical (HeLa, SiHa, and C33A), ovarian (A2780), and breast (MCF-7, MDA-MB-231, and T47D) cancer cells (Table 2). These test compounds, derived from 16α-azido-3-methoxyestra-1,3,5(10)-trien-17α-ol, feature a D-ring-fused oxazoline ring with a substituted 2′-phenyl group. Based on growth inhibition percentages and IC_{50} values, we determined that the test compounds displayed low to moderate antiproliferative activity across all examined cell lines. At a concentration of 30 μM, the compounds inhibited cell growth by approximately 70–80%. IC_{50} values were only determined for compounds I/6e and I/6g, as only these exceeded 75% inhibition at 30 μM: I/6e showed an IC_{50} value of 13.0 μM in HeLa cells, and I/6g showed an IC_{50} value of 16.5 μM in MCF-7 cells. No considerable differences in overall activity were observed between the compounds' effects on cervical, ovarian, or breast cancer cells.

4.1.2. 16-methylene-13α-estrone derivatives

In the present study, the *in vitro* antiproliferative activity of twelve newly synthesized 16-substituted, 13α-estrone-based α- and β-ketophosphine oxides (II/9–20) and their precursors (II/4 and II/5) were evaluated using a panel of human gynecological cancer cell lines, including cervical (HeLa, SiHa, and C33A), ovarian (A2780), and breast (MCF-7, MDA-MB-231, and T47D) cancer cells as well as oropharyngeal squamous cell carcinoma cell lines (UPCI-SCC-131 and UPCI-SCC-154). Non-cancerous mouse embryo fibroblast (NIH/3T3) cells were used to assess tumor selectivity (Table 3).

Comp.	Conc. (μM)	Growth inhibition; % ± SEM [calculated IC_{50} value; μM]						
		Hela	**SiHa**	**C33A**	**A2780**	**MCF-7**	**MDA-MB-231**	**T47D**
I/2	10	–	–	–	–	–	–	–
	30	31.46 ± 2.85	–	33.57 ± 1.81	26.16 ± 1.62	23.29 ± 2.10	34.70 ± 1.95	36.49 ± 2.46
I/6a	10	31.50 ± 1.68	–	–	–	20.22 ± 1.37	–	21.66 ± 2.55
	30	48.07 ± 1.69	34.45 ± 1.13	20.66 ± 1.98	–	45.05 ± 2.00	39.89 ± 2.47	48.30 ± 2.71
I/6b	10	–	–	–	–	–	–	–
	30	55.89 ± 0.59	23.94 ± 2.19	61.77 ± 2.70	31.71 ± 2.32	26.64 ± 3.05	30.94 ± 1.98	34.07 ± 2.36
I/6c	10	37.18 ± 2.99	36.10 ± 0.67	–	–	27.32 ± 2.93	38.88 ± 1.18	–
	30	62.30 ± 1.43	54.93 ± 0.91	23.18 ± 1.12	32.52 ± 2.38	50.62 ± 3.12	67.33 ± 1.80	43.47 ± 2.39
I/6d	10	–	–	–	–	–	–	–
	30	49.50 ± 0.96	28.14 ± 1.54	42.38 ± 2.67	–	49.46 ± 0.57	36.20 ± 1.41	49.70 ± 0.48
I/6e	10	35.02 ± 2.41	48.83 ± 1.81	24.38 ± 2.26	28.65 ± 1.44	51.30 ± 2.03	38.98 ± 1.25	49.10 ± 2.62
	30	76.75 ± 1.12 **[12.97]**	67.91 ± 1.15	50.34 ± 1.40	43.57 ± 3.10	71.07 ± 1.39	68.75 ± 1.15	73.70 ± 1.31
I/6f	10	–	29.73 ± 0.69	–	–	23.68 ± 1.03	35.02 ± 1.94	28.24 ± 2.48
	30	43.68 ± 3.11	53.05 ± 1.11	39.65 ± 2.26	33.91 ± 3.18	51.78 ± 1.47	60.63 ± 2.30	45.20 ± 1.29
I/6g	10	32.88 ± 1.43	43.04 ± 2.13	28.87 ± 2.91	34.55 ± 2.60	42.88 ± 2.08	22.39 ± 1.24	39.00 ± 1.76
	30	52.03 ± 2.63	72.61 ± 1.79	46.62 ± 2.52	65.92 ± 2.27	80.76 ± 1.46 **[16.52]**	35.54 ± 1.98	72.66 ± 1.94
CIS	10	42.61 ± 2.33	88.64 ± 0.50	85.98 ± 1.05	83.6 ± 1.2	66.91 ± 1.81	–	51.00 ± 2.02
	30	99.93 ± 0.26 [12.43]	90.18 ± 1.78 [7.84]	98.66 ± 0.21 [4.13]	95.0 ± 0.3 [1.30]	96.80 ± 0.35 [5.78]	71.47 ± 1.20 [19.13]	57.95 ± 1.45 [9.78]

Table 2: Antiproliferative activity of the tested estrone 16α,17α-oxazoline derivatives (–: Growth inhibition is less than 20%)

Comp.	Conc. (µM)	Growth inhibition; % ± SEM [calculated IC_{50} value; µM]									
		UPCI-SCC-131	UPCI-SCC-154	Hela	SiHa	C33A	A2780	MCF-7	MDA-MB-231	T47D	NIH/3T3
II/4	10 30	99.80 ± 0.36 99.88 ± 0.39 [3.17]	97.29 ± 1.10 97.81 ± 0.65 [5.15]	85.11 ± 2.44 99.43 ± 0.28 [4.45]	97.44 ± 0.54 99.28 ± 0.42 [3.31]	99.57 ± 0.61 99.55 ± 0.39 [3.60]	96.90 ± 1.52 100.5 ± 0.22 [6.24]	99.52 ± 0.51 99.83 ± 0.44 [3.70]	99.97 ± 0.71 94.64 ± 2.26 [3.97]	99.68 ± 0.74 99.92 ± 0.71 [3.46]	101.1 ± 0.67 100.9 ± 0.71 [2.79]
II/5	10 30	99.54 ± 0.33 99.94 ± 0.44 [2.38]	96.40 ± 0.89 100.3 ± 0.82 [4.50]	75.07 ± 3.73 99.65 ± 0.25 [6.99]	98.98 ± 0.26 99.97 ± 0.42 [2.30]	93.88 ± 2.56 100.0 ± 0.23 [3.75]	94.85 ± 2.13 100.9 ± 0.18 [6.70]	99.70 ± 0.43 100.6 ± 0.31 [3.35]	97.15 ± 1.46 98.57 ± 0.89 [4.07]	100.2 ± 0.28 101.3 ± 0.47 [3.47]	100.8 ± 0.16 100.3 ± 0.25 [2.74]
II/9 (EDPO)	10 30	63.42 ± 1.41 99.35 ± 0.27 **[5.30]**	– 99.82 ± 1.48 [13.49]	– 97.59 ± 0.73 [12.90]	– 96.49 ± 1.24 [13.79]	– 97.85 ± 0.32 [13.32]	47.23 ± 2.75 98.99 ± 0.41 [11.74]	21.29 ± 2.79 93.08 ± 1.60 [13.67]	– 99.03 ± 0.73 [23.49]	57.45 ± 3.15 93.77 ± 0.55 **[7.20]**	– 96.55 ± 0.86 [20.44]
II/10	10 30	39.82 ± 1.36 72.93 ± 1.70	– 24.32 ± 2.84	– 21.53 ± 2.99	– –	21.96 ± 1.84 27.25 ± 1.85	– 64.25 ± 2.65	– 35.85 ± 3.30	– –	– 61.09 ± 1.06	ND
II/11	10 30	20.86 ± 1.67 62.45 ± 1.40	– 38.56 ± 2.60	– 23.80 ± 2.11	– 30.22 ± 2.99	– 40.26 ± 0.95	– 21.91 ± 2.63	– 37.06 ± 0.72	– –	24.70 ± 1.70 58.96 ± 1.38	ND
II/12	10 30	49.38 ± 2.06 90.01 ± 1.15 [14.18]	– 75.46 ± 1.84 [29.83]	– 96.39 ± 1.88 [13.62]	– 94.83 ± 1.48 [14.12]	– 97.68 ± 0.85 [13.63]	– 97.14 ± 0.55 [28.46]	– 90.19 ± 1.61 [16.42]	– 84.01 ± 2.61 [24.46]	31.38 ± 1.55 75.02 ± 1.65 [16.97]	– 48.34 ± 1.65 [30.85]
II/13	10 30	29.88 ± 1.21 97.02 ± 0.43 [12.28]	– 75.94 ± 1.93 [21.51]	– 95.69 ± 0.69 [14.34]	– 92.90 ± 0.85 [13.72]	– 96.31 ± 0.46 [14.51]	– 97.77 ± 0.35 [23.75]	– 84.92 ± 2.54 [14.75]	– 95.56 ± 0.67 [25.81]	26.68 ± 1.95 89.82 ± 0.68 [13.58]	– 89.76 ± 0.49 [19.27]
II/14	10 30	48.75 ± 1.50 97.29 ± 1.38 [10.92]	– 87.05 ± 1.16 [11.38]	– 99.14 ±0.37 [12.22]	– 92.97 ± 1.37 [11.75]	26.86 ± 2.13 101.1 ± 0.24 [10.93]	– 100.3 ± 0.22 [21.46]	– 89.98 ± 2.88 [14.37]	– 98.22 ± 0.39 [17.59]	22.60 ± 1.33 85.98 ± 1.51 [13.85]	– 52.71 ± 2.87 [29.64]
II/15	10 30	24.60 ± 1.39 60.22 ± 1.32	– 34.66 ± 1.36	– 27.44 ± 1.57	– –	– 26.94 ± 0.84	– 49.39 ± 2.06	– –	– –	39.07 ± 2.01 58.50 ± 0.80	ND
II/16	10 30	49.45 ± 2.27 67.44 ± 1.11	– 31.55 ± 2.41	– 31.83 ± 2.27	– –	– 59.09 ± 0.69	– 67.27 ± 3.04	– –	– –	23.63 ± 1.22 64.48 ± 1.60	ND
II/17	10 30	26.48 ± 1.70 45.31 ± 1.84	– 20.26 ± 2.69	– –	– –	– –	– –	– –	– –	– 27.12 ± 2.93	ND
II/18	10 30	46.39 ± 1.19 64.55 ± 1.29	– –	– –	– –	– 20.25 ± 1.01	– –	– –	– –	– –	ND
II/19	10 30	– 40.98 ± 2.94	34.27 ± 2.80 48.81 ± 2.15	30.96 ± 1.11 48.89 ± 0.90	23.24 ± 1.36 40.30 ± 2.00	28.08 ± 1.39 34.69 ± 1.70	– 28.51 ± 2.35	31.84 ± 2.47 40.60 ± 1.71	– –	59.44 ± 2.44 62.41 ± 1.70	ND
II/20	10 30	48.25 ± 1.46 61.12 ± 1.32	30.97 ± 2.54 28.72 ± 1.11	– –	– –	27.94 ± 0.89 26.53 ± 1.06	– –	28.24 ± 1.66 22.21 ± 2.78	– –	66.09 ± 0.76 68.56 ± 1.81	ND
CIS	10 30	95.63 ± 1.49 95.09 ± 1.57 [1.22]	87.40 ± 1.72 92.72 ± 1.67 [1.29]	42.61 ± 2.33 99.93 ± 0.26 [12.43]	88.64 ± 0.50 90.18 ± 1.78 [7.84]	85.98 ± 1.05 98.66 ± 0.21 [4.13]	83.6 ± 1.2 95.0 ± 0.3 [1.30]	66.91 ± 1.81 96.80 ± 0.35 [5.78]	– 71.47 ± 1.20 [19.13]	40.41 ± 1.25 56.84 ± 1.16 [19.24]	76.74 ± 1.26 96.90 ± 0.25 [4.73]

Table 3: Antiproliferative activity of the tested 16-methylene-13α-estrone derivatives (–: Growth inhibition is less than 20%; ND: not determined)

Based on the calculated IC_{50} values (if determined), the precursor molecules II/4 and II/5 demonstrated high antiproliferative activity (IC_{50}: 2.30–6.99 μM) against all tested cell lines. In most cancer cell lines, the growth-inhibitory effects of these compounds were similar to those of the positive control, cisplatin. However, in the cases of HeLa, SiHa, and MDA-MB-231 cells, compounds II/4 and II/5 demonstrated greater potency, with IC_{50} values 2-5 times lower. Conversely, these agents also suppressed the proliferation of non-cancerous cells at concentrations comparable to those required for cancer cells, indicating a lack of tumor selectivity.

In the case of the C-16 substituted derivatives of the precursor molecules, marked differences can be observed in their antiproliferative potential against the tested cell lines. The twelve phosphine oxide derivatives were divided into three structural groups according to their C-16 substituents:

1) Di(naphthalen-2-yl) derivatives (II/17–20): Compounds II/17 and II/18 (3-methoxy derivatives) displayed negligible growth inhibition on most cell lines but showed relatively higher activity against UPCI-SCC-131 cells. The corresponding 3-benzyloxy analogues (II/19, II/20) demonstrated stronger antiproliferative effects, particularly against T47D breast cancer cells.

2) Di-*para*-tolyl derivatives (II/13–16): Among these, the 3-benzyloxy derivatives (II/15 and II/16) showed moderate activity, while the 3-methoxy analogues (II/13 and II/14) were among the four most potent phosphine oxides, with IC_{50} values between 10 and 25 μM. Their activity was strongest on UPCI-SCC-131 and T47D cells. Importantly, their IC_{50} values on NIH/3T3 cells (19.27 μM and 29.64 μM, respectively) were higher than on most cancer cell lines, indicating improved tumor selectivity compared to parent compound II/4.

3) Diphenyl derivatives (II/9–12): The 3-methoxy-16α-isomer, compound II/9 (EDPO) showed the most significant antiproliferative activity against the UPCI-SCC-131 and T47D cell lines, with IC_{50} values of 5.3 and 7.2 μM, respectively. EDPO also demonstrated substantial tumor selectivity, showing an IC_{50} value of 20.44 μM on NIH/3T3 cells that was approximately four times higher than on UPCI-SCC-131 cells and three times higher than on T47D cells. The 3-benzyloxy compounds (II/11 and II/12) displayed differing activities depending on the orientation of their substituents; compound II/12 (16β-isomer) was more active overall, though less selective.

After a thorough examination of the results of the MTT assay, we have shifted our focus to the most effective compound, EDPO. The test compound, which exerted a substantial inhibitory effect on the proliferation of the ERα+ T47D and UPCI-SCC-131 cells, also demonstrated a moderate inhibitory effect against the ERα+ MCF-7 cells (IC_{50} = 13.7 μM), and relatively low inhibitory effect on MDA-MB-231 triple-negative breast cancer cells (IC_{50} = 23.5 μM). Notably, EDPO displayed up to 1.50-, 2.83- and 3.85-fold greater potency against MCF-7, T47D and UPCI-SCC-131 cells, respectively, in comparison to its effect on non-cancerous mouse fibroblast cells (NIH/3T3; IC50 = 20.4 μM), indicating substantial tumor selectivity. These results demonstrate that EDPO may selectively inhibit the proliferation of ERα+ cancer cells. Based on these results, where we observed a negative correlation between ERα-positivity and the IC_{50} value of EDPO measured on the breast cancer cell lines, we hypothesized that our compound may exert its effect through the ERα-signaling.

4.2. Luciferase reporter gene assay

To address our hypothesis, the antiestrogenic properties of the investigational compound EDPO were evaluated in comparison with fulvestrant using the T47D-KBluc cell line, which harbors an integrated estrogen-responsive luciferase reporter. To further explore structure-activity relationships, effects of 3-BEDPO on transcriptional activity was also examined over the same concentration range. Preliminary experiments established 3.5×10^{-11} M E2 as the concentration inducing maximal transcriptional activation. The concentrations required to achieve 50% inhibition of ERα-mediated transcription (IC_{50} values) were determined to be 10^{-9} M for fulvestrant and 10^{-5} M for EDPO, whereas an IC_{50} value could not be determined for 3-BEDPO within the applied concentration range (Fig. 3). Collectively, these findings indicate that EDPO, but not 3-BEDPO, acts as an effective ERα antagonist, displaying a concentration-dependent inhibitory profile comparable to that of fulvestrant.

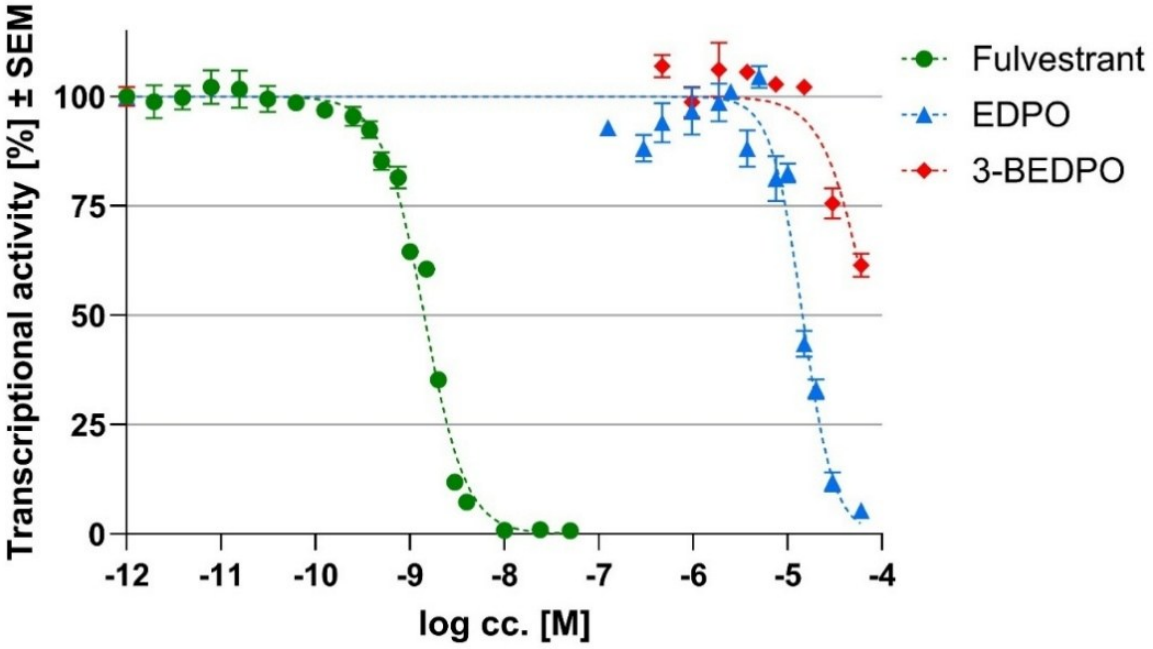

Figure 3: Concentration-response curves for the inhibition of ERE-Luciferase by fulvestrant, EDPO, and 3-BEDPO. T47D-KBluc cells were treated and co-incubated with E2 and the test compounds for 24 hours. Data points represent the mean ± SEM of at least three independent experiments.

4.3. *In vivo* uterotrophic assay

In this study, the antiestrogenic activity of EDPO was evaluated using an *in vivo* uterotrophic bioassay in a rodent model. Administration of E2 (0.1 µg/g) produced an approximately 6-fold increase in uterine weight relative to the vehicle control group. Co-treatment with fulvestrant (0.3 µg/g) reduced the E2-induced uterine hypertrophy by about 50%. Comparable to fulvestrant, EDPO significantly attenuated E2-driven uterine growth in a dose-dependent manner. Uterine weights in all test groups differed significantly from those in the positive control group, treated with E2 alone. Moreover, significant differences were observed between the lower EDPO dose and the fulvestrant group, as well as between the low- and high-dose EDPO groups, whereas no significant difference was detected between the fulvestrant-treated group and the higher EDPO dose group (Fig. 4A). Consistent with these quantitative findings, pronounced macroscopic differences in uterine morphology were evident among the treatment groups (Fig. 4B). Collectively, these results demonstrate that EDPO effectively suppresses ER-mediated uterine tissue growth *in vivo*.

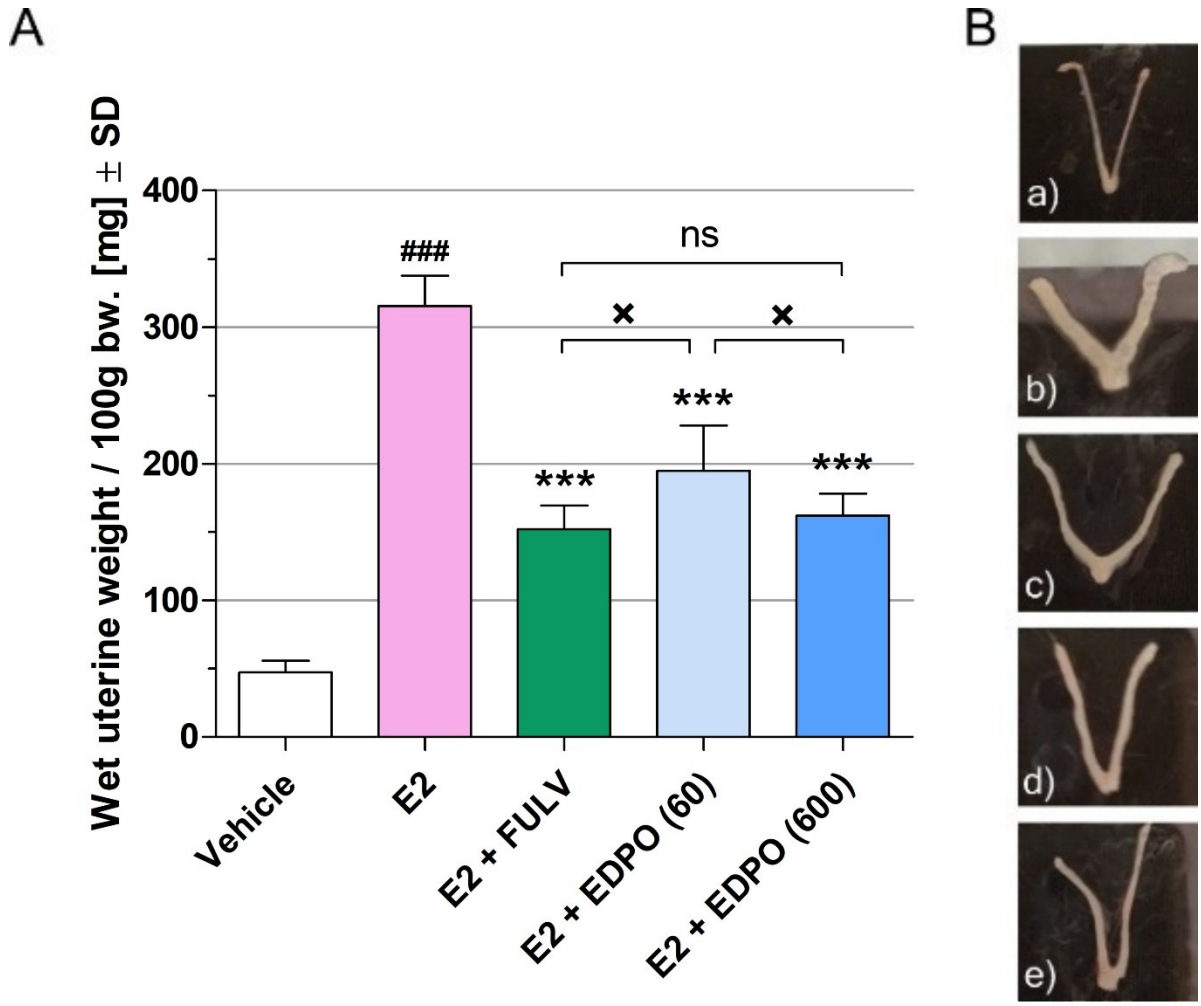

Figure 4: Effects of fulvestrant and EDPO on uterine weight of female, immature Sprague-Dawley rats. A: Wet uterine weights are represented as mean ± SD in mg normalized for 100 g of animal body weight. One-way ANOVA was used for statistical analysis, and significant differences are indicated with ### at $p < 0.001$ vs. vehicle group; *** at $p < 0.001$ vs. E2 group; × at $p < 0.05$ for E2 + FULV vs. E2 + EDPO (60) and E2 + EDPO (60) vs. E2 + EDPO (600) group; ns: not significant, (n = 6). **B:** Uterine appearances in response to (a) vehicle, (b) E2 (0.1 µg/g), (c) E2 (0.1 µg/g) + FULV (0.3 µg/g), (d) E2 (0.1 µg/g) + EDPO (60 µg/g) and (e) E2 (0.1 µg/g) + EDPO (600 µg/g).

4.4. Cell cycle analysis

To evaluate the effect of EDPO on cell cycle dynamics, propidium iodide-based flow cytometric analysis was conducted using the T47D cell line. Cells were treated with increasing concentrations of the test compound, and with fulvestrant (5 µM) included as a positive control. The data revealed clear time- and concentration-dependent effects. EDPO treatment resulted in cell cycle arrest at the G1 phase, as demonstrated by a significant expansion of the G1 population and a concomitant reduction in the S-phase fraction across all investigated time points. This G1 phase arrest was most evident after 24 hours of exposure, during which a pronounced accumulation of cells in the G1 phase was observed at every concentration tested. (Fig. 5).

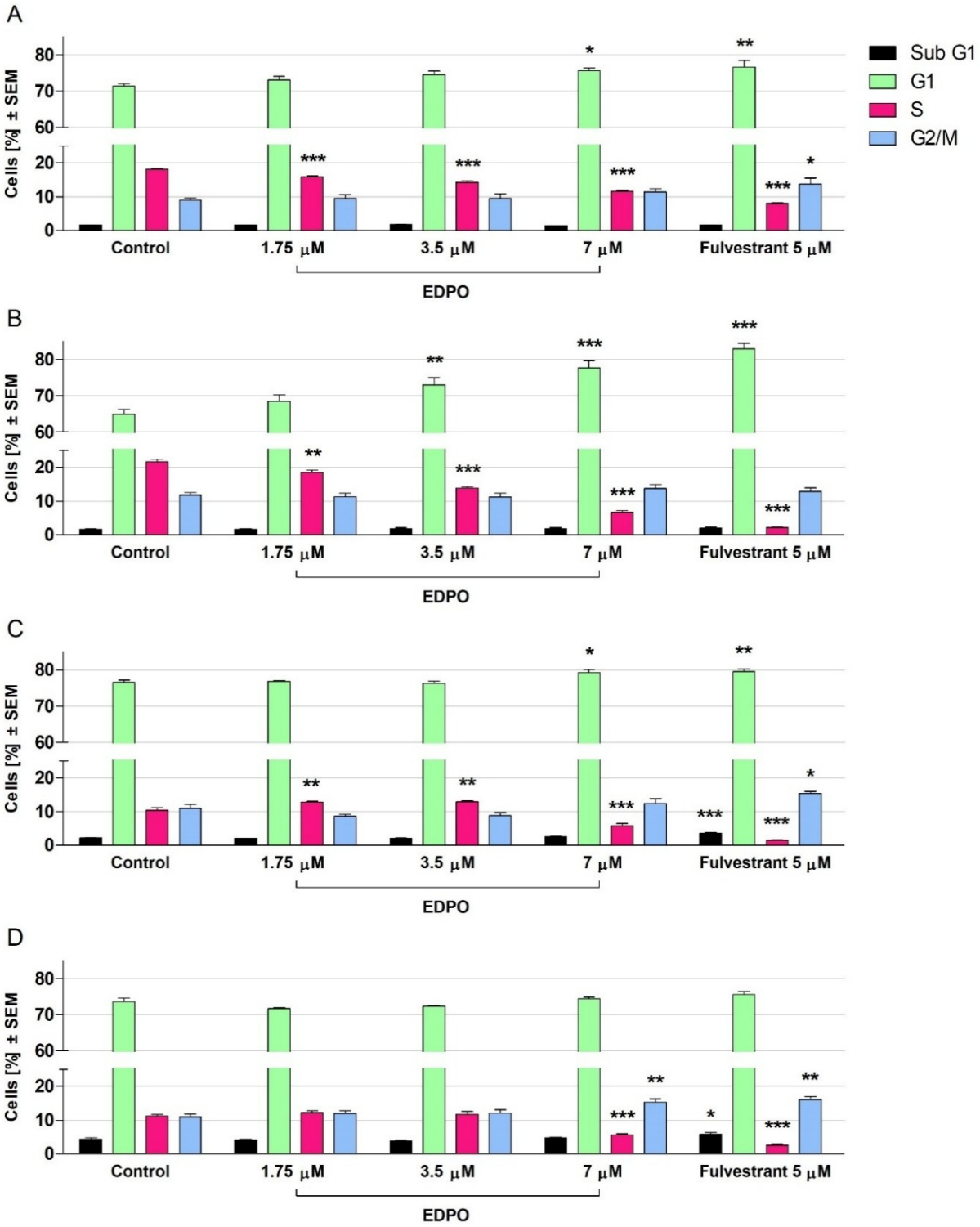

Figure 5: EDPO-induced cell cycle disturbance in the G1 phase compared to fulvestrant observed after 12 (A), 24 (B), 48 (C), and 72 hours (D) of incubation on T47D cells. One-way ANOVA was used for statistical analysis, with *, **, and *** indicating significance at $p < 0.05$, $p < 0.01$, and $p < 0.001$, respectively, compared to the non-treated control samples. Results are from at least two independent experiments performed in quadruplicates.

4.5. Cell migration (wound healing) assay

To assess the antimigratory potential of EDPO, a wound healing assay was conducted in UPCI-SCC-131 and T47D cell lines under serum-reduced conditions (2% FBS). Migration was quantified by image-based measurement of the cell-free area at 0, 24, and 48 hours following exposure to the compound. Despite the marked differences in migratory capacity between the two cell lines, EDPO treatment significantly impaired cell migration in both UPCI-SCC-131 and T47D cells. In UPCI-SCC-131 cells, significant inhibition was observed at both tested concentrations after 24 hours of treatment, whereas at 48 hours, only the higher concentration produced a statistically significant reduction in migration (Fig. 6).

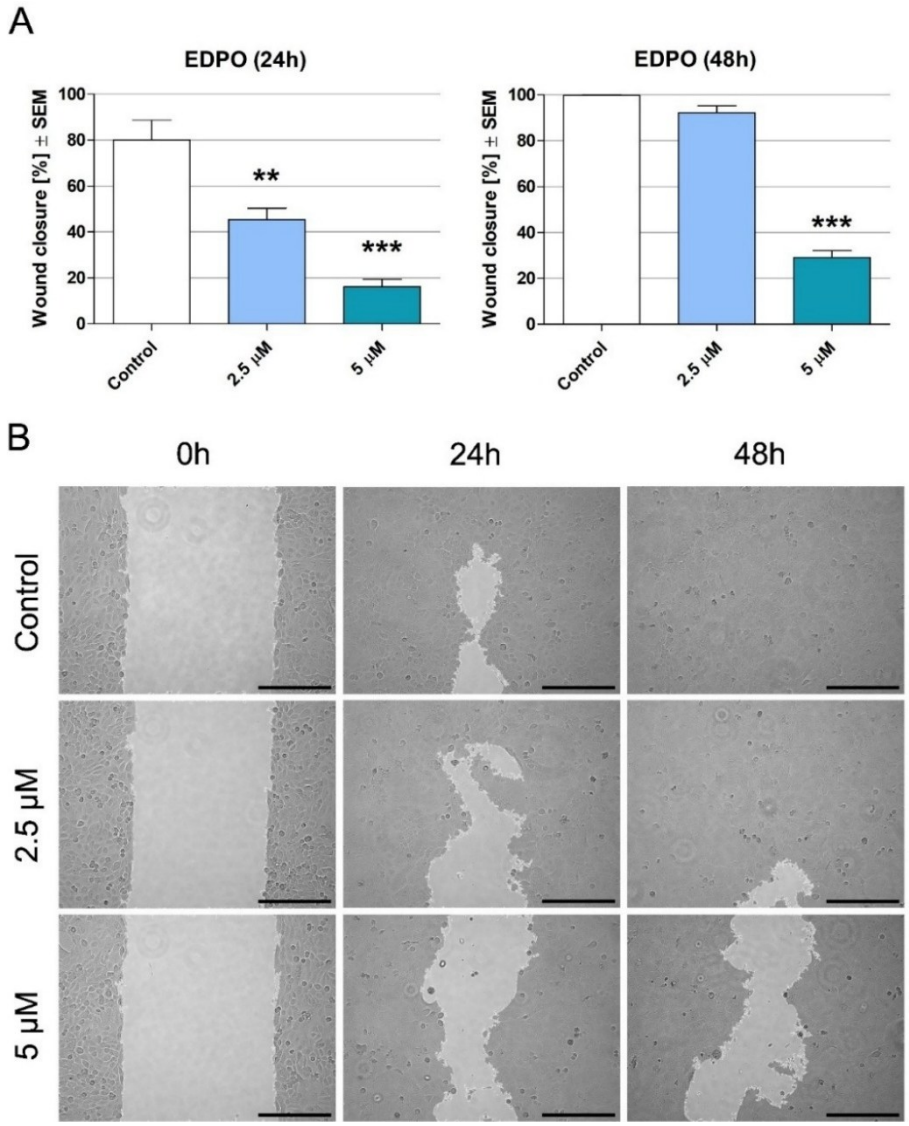

Figure 6: Antimigratory effect of EDPO measured by wound healing assay. A: Effects of EDPO on UPCI-SCC-131 cell migration after 24 and 48 hours of incubation. One-way ANOVA was used for statistical analysis, with ** and *** indicating significance at $p < 0.01$ and $p < 0.001$, respectively, compared to the non-treated control samples. Results are from at least two independent experiments performed in quadruplicates. **B:** Representative images of the antimigratory effects of EDPO after 0, 24, and 48 hours of incubation. Scale bar: 250 µm

In contrast, the T47D cell line showed less pronounced alterations in migratory behavior following treatment; however, these changes remained statistically significant at both concentrations and across all incubation periods examined (Fig. 7). Overall, these data demonstrate that EDPO markedly reduces the migratory capacity of the analyzed tumor cell lines in a time- and dose-dependent manner.

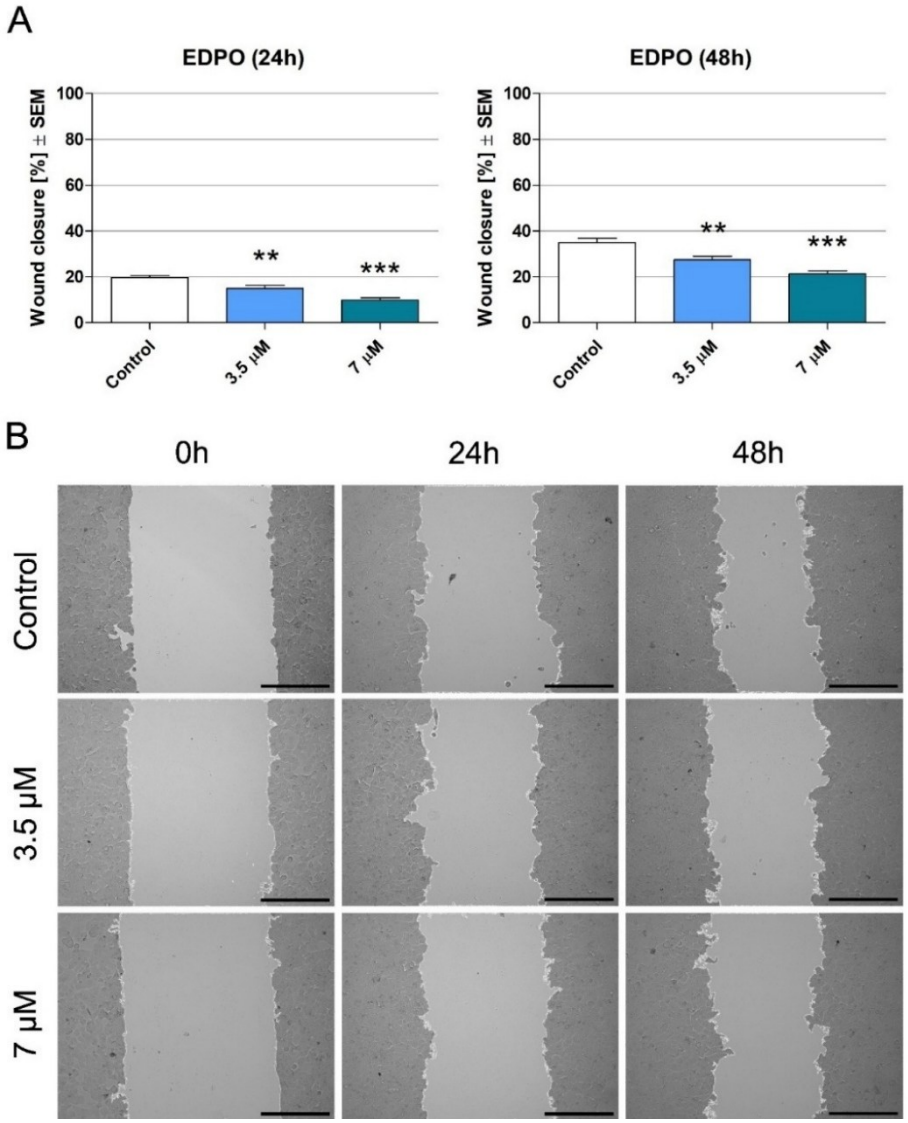

Figure 7: Antimigratory effect of EDPO measured by wound healing assay. A: Effects of EDPO on T47D cell migration after 24 and 48 hours of incubation. One-way ANOVA was used for statistical analysis, with ** and *** indicating significance at $p < 0.01$ and $p < 0.001$, respectively, compared to the non-treated control samples. Results are from at least two independent experiments performed in quadruplicates. **B:** Representative images of the antimigratory effects of EDPO after 0, 24, and 48 hours of incubation. Scale bar: 250 µm

4.6. Transwell invasion (Boyden chamber) assay

The antimetastatic potential of EDPO was evaluated using a transwell migration assay in the T47D cell line. Whole-membrane imaging was performed, and cellular invasion was quantified based on the invaded area. Compared to untreated controls, EDPO treatment resulted in a significant decrease in invasive capacity at both tested concentrations. Specifically, the compound reduced the extent of cell invasion to approximately 50% of control levels; however, this inhibitory effect did not display a statistically significant dose-dependent trend (Fig. 8).

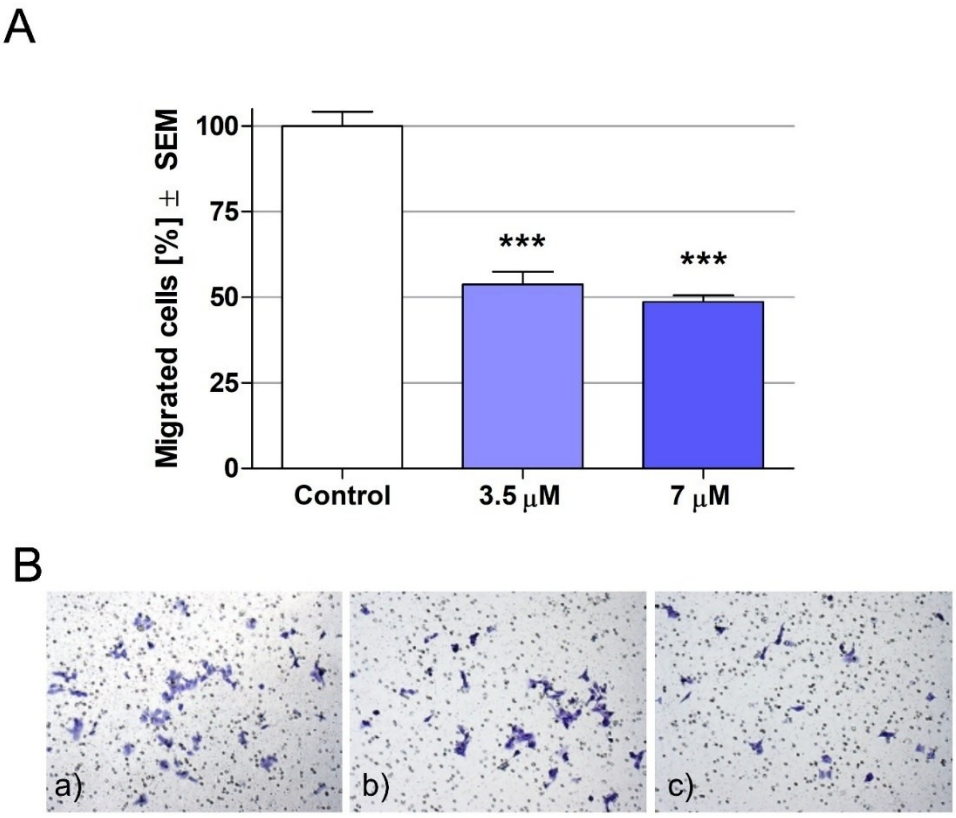

Figure 8: Effect of EDPO on the invasive capacity of T47D cells measured by transwell migration (Boyden chamber) assay. A: Effect of EDPO on T47D cell invasion after 48 hours of incubation. One-way ANOVA was used for statistical analysis, with *** indicating significance at $p < 0.001$, compared to the non-treated control samples. Results are from at least two independent experiments performed in duplicates. **B:** Representative images of the non-treated samples (a) and the anti-invasive effects of EDPO at 3.5 μM (b) and 7 μM (c) concentration after a 48-hour incubation period.

5. Discussion

Estrogen receptor-positive breast cancer accounts for roughly 70% of breast malignancies and remains fundamentally driven by estrogen signaling through ERα, which regulates genes involved in cell proliferation, survival, and metastatic progression. Although endocrine therapies such as SERMs, AIs, and SERDs have substantially reduced mortality and recurrence risk, intrinsic and acquired resistance is pervasive and limits long-term efficacy. Up to 30-50% of patients relapse despite initial responsiveness, reflecting adaptive changes in receptor signaling, engagement of alternative proliferative pathways, and modifications in ERα itself that allow tumor growth independent of classical estrogen stimulation [71,72].

Endocrine resistance arises through multiple, often interconnected processes: hypersensitivity of ER to low estrogen levels, ligand-independent receptor activation, alterations in coactivator/corepressor interactions, and crosstalk with growth factor pathways, all of which contribute to sustained proliferative signaling despite blockade of conventional estrogen pathways [73]. These adaptations are compounded by the selective pressure exerted by prolonged hormone therapy, promoting cell populations that bypass estrogen dependence or exploit compensatory survival mechanisms.

Concurrently, the clinical landscape demonstrates that even next-generation targeted endocrine agents, including oral SERDs and combination regimens (*e.g.*, CDK4/6 or PI3K inhibitors), while advancing progression-free survival, do not fully eliminate resistance or recurrence risk, and often add significant toxicity [74]. This ongoing challenge underscores the need for therapeutics that retain or enhance anti-ER activity while mitigating pathways of resistance and systemic adverse effects.

Rational design of novel steroid-based compounds may offer a compelling strategy to address these issues. Structural modification of steroid scaffolds can theoretically yield agents that inhibit ERα-signaling (even through non-canonical pathways), suppressing proliferative transcriptional programs, evading receptor mutations, and interacting with auxiliary targets involved in survival and metastatic phenotypes. Unlike traditional SERMs or AIs, such compounds may combine receptor antagonism with unique pharmacodynamic profiles, potentially reducing compensatory activation of alternative pathways driving endocrine escape.

In the present study, two sets of D-ring modified estrone-derivatives were employed to assess their antiproliferative efficacy against various female breast, gynecological and oropharyngeal cell lines. The most effective derivative, compound II/9 (EDPO) was assayed

using other *in vitro* and *in vivo* methodologies in order to determine its possible mechanism of action.

The growth inhibition data allowed for the ranking of compound efficacy within each of the investigated cell lines, revealing structure-activity relationships among the azido alcohol derivatives I/6a–6g. In general, converting the azido alcohol I/2 into a D-ring-fused oxazoline slightly enhanced antiproliferative activity; for example, compound I/6a in HeLa cells. Additionally, halogen substitution on the phenyl ring (compounds I/6b, I/6c, and I/6d) improved activity, particularly in HeLa and C33A cells. Among these, chlorine substitution resulted in the greatest enhancement across multiple cell lines.

The most pronounced antiproliferative effects were observed in compounds bearing 4″-nitrile, 4″-nitro, or 4″-methoxy substituents, as these appeared most frequently among the top three most active compounds in each cell line (three, six, and seven occurrences, respectively). Compound I/6g (with a 4″-nitro group) was most effective against SiHa, A2780, and MCF-7 cells, while compound I/6e (bearing a 4″-methoxy group) showed the highest activity against HeLa and MDA-MB-231 cells. Notably, the IC_{50} of I/6e on HeLa cells (12.9 μM) was comparable to that of cisplatin (12.4 μM), a clinically used positive control for gynecological cancers. Both I/6e and I/6g demonstrated similar efficacy in T47D breast cancer cells.

In summary, while the synthesized D-ring-fused 2′-phenyl oxazoline derivatives of 16α,17α-azido alcohol I/2 exhibited only moderate antiproliferative effects on gynecological cancer cell lines, systematic chemical modifications of the D-ring-fused 2′-phenylestrane scaffold significantly influenced biological activity. Among them, the 4″-methoxy-substituted compound I/6e stands out as a promising lead for the development of novel estrane-based anticancer agents with enhanced potency. While these current findings are encouraging, due to the limited number of analogues evaluated, it cannot be stated with high confidence that this type of modification on the D-ring favorably influences the extent of the antiproliferative effect. Investigation of a broader and more diverse molecular library would be required to validate this structure-activity relationship.

Concerning the biological properties of the 16-methylene-13α-estrone derivatives, the results indicate that modifications at the C-3, C-16, and C-17 positions of the 13α-estrone scaffold significantly influence both cytostatic potency and tumor selectivity. Consistent with our findings, the presence of a 3-methoxy substituent was shown to be beneficial for antiproliferative activity and selectivity.

Among the tested compounds, II/9 (EDPO) exhibited the most favorable combination of activity and selectivity, with IC_{50} values comparable to cisplatin on UPCI-SCC-131 and

T47D cells. The presence of bulky substituents such as naphthyl groups at C-16 substantially reduced antiproliferative potency, likely due to steric effects interfering with molecular interactions. In contrast, the orientation of smaller substituents (*para*-tolyl or phenyl) had minimal influence, suggesting that steric bulk, rather than stereochemistry, primarily determines biological activity at this site.

The consistent sensitivity of UPCI-SCC-131 and T47D cells to several phosphine oxide derivatives suggests potential cell line-specific susceptibility linked to their molecular profiles. Overall, these findings highlight that targeted modifications at the A- and D-rings of the 13α-estrone core, particularly introduction of a 3-methoxy group, can yield cytostatic agents with improved selectivity. Moreover, after a thorough examination of the results, we also concluded that the lead compound of the series (EDPO) emerged as particularly promising, displaying low micromolar IC_{50} values in the ERα-positive T47D and MCF-7 breast cancer cell lines, while its efficacy was markedly reduced, by approximately 3.3 and 1.7-fold, respectively, in the triple-negative MDA-MB-231 cell line, which lacks ERα expression [75]. This differential sensitivity suggested that the presence of ERα may contribute to the compound's mechanism of action. The selective potency toward ERα-positive models therefore provided a strong rationale to hypothesize that the compound may exert its antiproliferative effects, at least in part, through modulation of the estrogen receptor signaling pathway. This conclusion guided the design and implementation of subsequent experiments aimed at elucidating the compound's suspected mechanism of action.

Estrogen and ERα are central regulators in the onset and progression of ER^+ breast cancers. The ERα signaling cascade controls the transcription of numerous genes involved in cell proliferation, differentiation, and survival [76]. Consequently, interference with this pathway at various molecular stages has been established as an effective therapeutic strategy to counteract estrogen-driven tumor growth and metastasis.

To investigate the impact of different compounds on ERα-mediated transcriptional activity, the T47D-KBluc reporter cell line was employed. This cell model is designed to quantitatively assess the modulation of estrogen receptor signaling through a luciferase reporter gene under the control EREs [77]. In this system, the compound EDPO demonstrated a clear inhibitory effect on E2-induced transcriptional activation, comparable to that of the well-characterized antiestrogen fulvestrant. This indicates that EDPO efficiently suppresses ERα-dependent gene expression. In contrast, its structural analog 3-BEDPO, which carries a 3-benzyloxy substitution, exhibited a substantially weaker antagonistic activity as measured by

the luminometric assay. This reduced efficacy aligns well with its lower antiproliferative potential observed in T47D breast cancer cells.

The uterotrophic assay in immature rats is a widely accepted *in vivo* model for evaluating the estrogenic or antiestrogenic properties of compounds [50]. In this study, we showed that EDPO reduces E2-induced uterine growth in a dose-dependent manner. The observed decrease in uterine weight indicates that EDPO effectively mitigates ERα activity under physiological conditions, demonstrating a potency similar to that of a well-established chemotherapeutic agent.

In our latest report, in collaboration with Hetényi and colleagues (Pharmacoinformatics Unit, Department of Pharmacology and Pharmacotherapy, Medical School, University of Pécs), the computational model of molecular docking of EDPO to ERα was also discussed. The *in silico* experimental results demonstrated that EDPO and fulvestrant display comparable binding profiles to ERα [79]. In the natural ligand (E2)–hERα complex, Helix 12 (H12) stabilizes in an agonistic conformation that enables coactivator binding and transcriptional activation [80–82]. In contrast, SERMs and SERDs such as raloxifene and fulvestrant disrupt this configuration by forming hydrogen bonds that displace H12, thereby blocking coactivator interaction and inducing antiestrogenic effects [80,82]. Docking results showed that fulvestrant and EDPO form similar stabilizing H-bonds with residues E353 and R394, crucial for ligand affinity and receptor stabilization [83], while 3-BEDPO lacks these key interactions. Moreover, EDPO forms an additional H-bond with T347, which may further prevent the agonistic positioning of H12 [84]. In contrast, 3-BEDPO's weaker van der Waals interactions likely fail to disrupt the receptor's active conformation, explaining its lack of antiestrogenic activity [79].

Taken together, findings from the three complementary approaches provide strong evidence that EDPO mediates its antiestrogenic activity by interfering with the ERα and its downstream signaling pathway.

It is well established that estrogen-driven cell proliferation is mediated by the rapid upregulation of key cell cycle regulators such as Cyclin D1, MDM2, and the early activation of the proto-oncogene c-Myc, all of which play crucial roles in facilitating the transition through the G1/S checkpoint [85–87]. Cyclin D1, when complexed with CDK4/6, phosphorylates the retinoblastoma protein (pRb), leading to the release of E2F1 and subsequent transcriptional activation of genes required for S-phase entry, including Cyclin E [88]. Cyclin E then associates with CDK2, further phosphorylating pRb and amplifying E2F1-mediated transcription [89].

In opposition to these proliferative signals, the p53–p21 pathway acts as a key regulatory checkpoint. Upon genotoxic stress, p53 activates the transcription of p21, which inhibits the Cyclin D1–CDK4/6 and Cyclin E–CDK2 complexes, thereby maintaining pRb in its hypophosphorylated, growth-suppressive state and halting E2F1-driven G1/S progression [90]. Conversely, c-Myc promotes cell cycle progression by repressing p21 expression, thereby sustaining cyclin-CDK activity at the G1/S boundary. Meanwhile, the human homolog of murine double minute 2 (MDM2), which is generally overexpressed in tumors, acts as a negative regulator of p53, promoting the degradation of pRb and p21 while also enhancing E2F1 activity [87].

Previous research demonstrated that fulvestrant decreases MDM2 protein levels by enhancing its turnover, ultimately resulting in G1 phase arrest [69]. In our experiments, both EDPO and fulvestrant similarly induced pronounced G1 arrest in T47D cells. Together with our earlier findings, these results further substantiate the antiestrogenic character of EDPO, suggesting that its inhibitory effect on cell proliferation may be mediated through disruption of this cell cycle regulatory network (Fig. 9A).

In ERα$^+$ breast cancer, E2 not only promotes cell proliferation but also induces morphological changes that enhance cellular motility and invasiveness through ERα-dependent signaling [91]. Mechanistically, activation of ERα initiates a Gαi/Gβγ-mediated signaling cascade that promotes the assembly of a multiprotein complex consisting of ERα, c-Src, phosphoinositide 3-kinase (PI3K), and focal adhesion kinase (FAK). This interaction results in the phosphorylation of FAK, which subsequently activates neural Wiskott-Aldrich syndrome protein (N-WASP). At the same time, PI3K catalyzes the production of phosphatidylinositol-3,4,5-trisphosphate (PIP3), promoting the recruitment and activation of cdc42. Once activated, cdc42 cooperates with phosphatidylinositol-4,5-bisphosphate (PIP2) to further stimulate N-WASP, which in turn regulates the actin-related protein 2/3 (Arp2/3) complex, driving actin filament branching and plasma membrane remodeling [92] (Fig. 9B). These cytoskeletal rearrangements are essential for the migratory and invasive behavior of cancer cells, particularly in ERα$^+$ breast tumors. Given that enhanced migration and invasion of cancer cells underpin metastatic progression, the primary cause of cancer-related mortality, agents that effectively inhibit these processes represent promising candidates for anticancer therapy.

Previous studies have shown that antiestrogenic agents can effectively suppress ERα-mediated migration and invasion of breast cancer cells [93]. Moreover, ERα has been detected and found to be functionally active in head and neck squamous cell carcinoma (HNSCC) cell lines, where it contributes to their proliferative and invasive properties [94]. Considering that

ERα-dependent FAK phosphorylation and focal adhesion turnover are pivotal for cancer cell motility, the inhibitory effects observed for our compound likely result from interference with these signaling mechanisms. This suggests that EDPO holds therapeutic potential for limiting the progression and metastatic spread of both ER^+ breast cancer and HNSCC.

Moreover, in collaboration with Puskás and colleagues (Avidin Ltd., Szeged), it was also established that EDPO effectively inhibits tumor growth in a 4T1 murine TNBC model [79]. While ERα-negative cancers, including triple-negative breast cancers (TNBCs), are traditionally considered estrogen-insensitive, recent studies show that estrogens modulate the immune environment to promote tumor progression. In the bone marrow, E2 drives myeloid progenitors to differentiate into myeloid-derived suppressor cells (MDSCs), which migrate to the tumor microenvironment (TME) and suppress cytotoxic T lymphocyte (CTL) activity [95,96]. Estrogens can also directly inhibit CTLs by blocking the autocrine interleukin-2 signaling. In a 4T1 TNBC mouse model, blocking estrogen signaling with fulvestrant decreased tumor growth, increased CTL infiltration, and shifted the TME toward a pro-immunogenic state with elevated effector molecules like granzyme B, perforin 1, and interferon-γ [96]. The previously described antitumor effect of EDPO can be explained by this mechanism (Fig. 9C).

In conclusion, our findings highlight a rational strategy for the development of targeted anticancer agents based on structurally modified estrone derivatives. In particular, the emphasis on D-ring modifications provides a promising framework for drug design, offering new opportunities to generate effective therapeutic candidates against both hormone-dependent and hormone-independent malignancies.

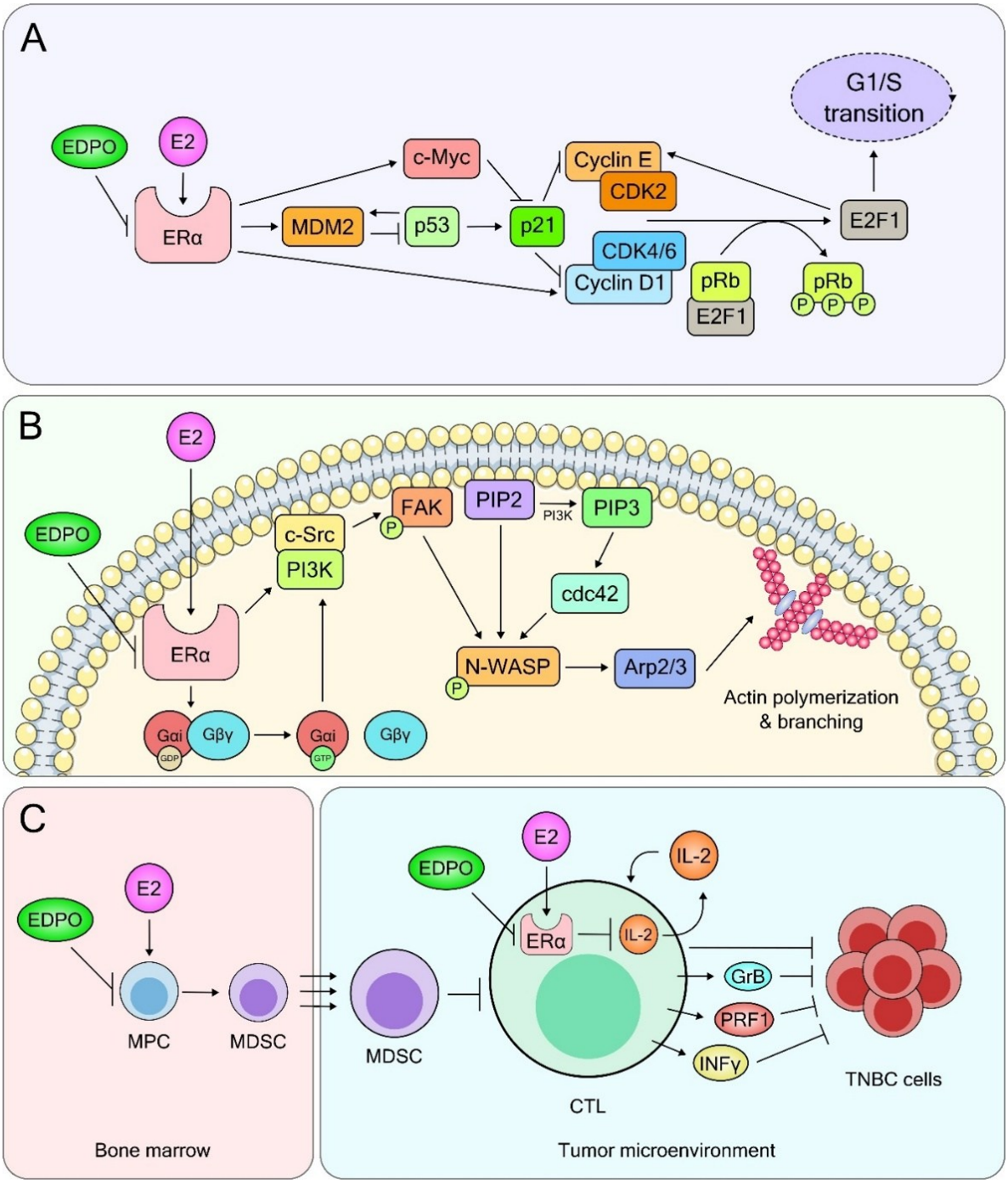

Figure 9: Proposed mechanism of action of EDPO on ERα+ and triple-negative breast cancer (TNBC) based on experimental and literature data. A: *Antiproliferative effect against ERα+ breast cancer cells.* Estrogen signaling drives G1/S transition by inducing Cyclin D1 and c-Myc, ultimately activating cyclin–CDK complexes to inactivate pRb and release E2F1, while simultaneously suppressing the p53-p21 axis through the induction of MDM2. EDPO may counteract this pathway by blocking ERα-driven transcription, reducing CDK activity, stabilizing p53, and restoring checkpoint control. **B:** *Antimetastatic effect against ERα+ breast cancer cells.* ERα promotes migration *via* non-genomic signaling, where estrogen-ERα activates G-proteins and c-Src, leading to PIP3 generation, FAK-mediated adhesion turnover, and Cdc42/Arp2/3-driven actin remodeling. This cascade reorganizes the cytoskeleton to enhance motility. EDPO is proposed to inhibit this ER-dependent pathway, thereby suppressing cell migration. **C:** *Antitumor effect against TNBC cells.* Estrogen-induced dual inhibitory action on CTLs through the mobilization of MDSCs and direct blockade of autocrine IL-2 signaling. EDPO is suggested to counteract the effects of E2, thereby shifting the tumor microenvironment toward a pro-immunogenic state and impairing tumor growth.

6. Summary

In this thesis, two distinct groups of D-ring-modified estrone derivatives, 16α,17α-oxazolines and 16-methylene-13α-estrone-based organophosphorus compounds were evaluated for their antiproliferative and antimetastatic potential in breast, gynecological, and oropharyngeal cancer models. Through a systematic comparison of structure-activity relationships, the aim of this work was to identify lead molecules with improved potency and tumor selectivity and to elucidate their possible mechanisms of action.

Initial viability assays demonstrated that several of the newly synthesized compounds exert moderate growth-inhibitory effects; however, among all derivatives tested, the organophosphorus compound II/9 (EDPO) emerged as the most promising candidate. EDPO displayed low micromolar IC_{50} values, particularly in ERα-positive breast cancer cell lines (T47D and MCF-7), while exhibiting markedly reduced activity in ER-negative models *in vitro*. This selectivity pattern strongly suggested that its mechanism of action may be linked to modulation of estrogen receptor signaling.

Subsequent mechanistic studies supported this hypothesis. In the T47D-KBluc reporter cell line, EDPO effectively suppressed estrogen-induced transcriptional activity in a concentration-dependent manner, exhibiting functional antagonism comparable to that of fulvestrant. Its antiestrogenic properties were further confirmed *in vivo*, where EDPO significantly reduced E2-induced uterine growth in a dose-dependent manner in the immature rat uterotrophic assay. These results demonstrate that EDPO interferes with ERα signaling under both experimental and physiological conditions.

Analysis of cell cycle distribution revealed that EDPO induces a pronounced G1 phase arrest, consistent with the inhibition of ER-mediated proliferative pathways. Furthermore, EDPO significantly impaired cancer cell motility and invasiveness in wound-healing and transwell assays, indicating additional antimetastatic potential. Complementary *in silico* docking studies suggested that EDPO forms key stabilizing interactions within the ERα ligand-binding domain, interactions that are absent in structurally related but biologically weaker analogs, providing a molecular explanation for its observed biological activity. Moreover, when employed in a rodent TNBC model, EDPO significantly suppressed tumor growth, likely by inhibiting estrogen signaling. Although TNBC is ERα-negative, estrogens promote tumor progression by suppressing antitumor immunity through MDSC expansion and direct inhibition of cytotoxic T lymphocytes. In line with this, estrogen blockade reduced tumor

growth, increased CTL infiltration, and induced a pro-immunogenic tumor microenvironment, providing a mechanistic explanation for EDPO's antitumor effect.

Overall, this work demonstrates that targeted chemical modification of the estrone scaffold can yield derivatives with improved anticancer efficacy and tumor selectivity. Among the tested compounds, EDPO emerges as a compelling lead with dual antiproliferative and antimetastatic properties mediated, at least in part, by ERα antagonism, offering a solid basis for further optimization of estrone-based antineoplastic agents.

7. Glossary of Acronyms and Abbreviations

- **ANOVA:** analysis of variance
- **Arp2/3:** actin related protein 2/3
- **ATCC:** American Type Culture Collection
- **BRCA1/BRCA2:** breast cancer type 1 susceptibility protein / breast cancer type 2 susceptibility protein
- **CCD:** charge-coupled device
- **CIS:** cisplatin
- **CDK:** cyclin-dependent kinase
- **CTL:** cytotoxic T-lymphocyte
- **DMSO:** dimethyl sulfoxide
- **Comp.:** compound
- **Conc.:** concentration
- **E2:** 17β-estradiol
- **ECACC:** European Collection of Authenticated Cell Cultures
- **EDPO:** 3-methoxy-17-oxo-13α-estra-1,3,5(10)-trien-16α-yl)methyl]diphenylphosphin oxide
- **EMEM:** Eagle's minimal essential medium
- **ERE:** estrogen responsive element
- **ERα:** estrogen receptor alpha
- **FAK:** focal adhesion kinase
- **FBS:** fetal bovine serum
- **G1:** first growth phase of the cell cycle
- **G2/M:** second growth phase of the cell cycle / mitotic phase
- **GLOBOCAN:** Global Cancer Observatory
- **GrB:** granzyme B
- **IARC:** International Agency for Research on Cancer
- **IC_{50}:** half maximal inhibitory concentration
- **IL-2:** interleukin-2
- **INFγ:** interferon-γ
- **MDM2:** murine double minute 2 homolog protein
- **MDSC:** myeloid-derived suppressor cell

- **MPC:** myeloid progenitor cell
- **MTT:** 3-(4,5-dimethylthiazol-2-yl)-2,5-diphenyltetrazolium-bromide
- **ND:** not determined
- **N-WASP:** neural Wiskott-Aldrich syndrome protein
- **PBS:** phosphate-buffered saline
- **PET:** polyethylene terephthalate
- **PI:** propidium iodide
- **PI3K:** phosphatidylinositol 3-kinase
- **PIP2:** phosphatidylinositol 4,5-bisphosphate
- **PIP3:** phosphatidylinositol 4,5,6-trisphosphate
- **pRb:** retinoblastoma protein
- **PRF1:** perforin-1
- **RPMI 1640:** Roswell Park Memorial Institute 1640 medium
- **S:** synthetic phase of the cell cycle
- **SD:** standard deviation
- **SEM:** standard error of the mean
- **Sub-G1:** hypodiploid cell population

8. References

1. Bray F, Laversanne M, Sung H, Ferlay J, Siegel RL, Soerjomataram I, Jemal A. Global cancer statistics 2022: GLOBOCAN estimates of incidence and mortality worldwide for 36 cancers in 185 countries. *CA Cancer J Clin*. **74,** 229–263 (2024). https://doi.org/10.3322/caac.21834
2. Ma T, Weng Z, Zhou S, Feng L, Qin Z, Ma D. Global burden and regional inequalities of cancer in older adults from 1990 to 2021 and its projection until 2050. *BMC Public Health*. **25,** 3633 (2025). https://doi.org/10.1186/s12889-025-24910-7
3. Anand P, Kunnumakara AB, Sundaram C, Harikumar KB, Tharakan ST, Lai OS, Sung B, Aggarwal BB. Cancer is a Preventable Disease that Requires Major Lifestyle Changes. *Pharm Res*. **25,** 2097–2116 (2008). https://doi.org/10.1007/s11095-008-9661-9
4. Wu S, Zhu W, Thompson P, Hannun YA. Evaluating intrinsic and non-intrinsic cancer risk factors. *Nat Commun*. **9,** 3490 (2018). https://doi.org/10.1038/s41467-018-05467-z
5. De Martel C, Georges D, Bray F, Ferlay J, Clifford GM. Global burden of cancer attributable to infections in 2018: a worldwide incidence analysis. *Lancet Glob Health*. **8,** e180–e190 (2020). https://doi.org/10.1016/S2214-109X(19)30488-7
6. Daly MB, Pal T, Berry MP, Buys SS, Dickson P, Domchek SM, Elkhanany A, Friedman S, Goggins M, Hutton ML, CGC, Karlan BY, Khan S, Klein C, Kohlmann W, CGC, Kurian AW, Laronga C, Litton JK, Mak JS, LCGC, Menendez CS, Merajver SD, Norquist BS, Offit K, Pederson HJ, Reiser G, CGC, Senter-Jamieson L, CGC, Shannon KM, Shatsky R, Visvanathan K, Weitzel JN, Wick MJ, Wisinski KB, Yurgelun MB, Darlow SD, Dwyer MA. Genetic/Familial High-Risk Assessment: Breast, Ovarian, and Pancreatic, Version 2.2021, NCCN Clinical Practice Guidelines in Oncology. *J Natl Compr Canc Netw*. **19,** 77–102 (2021). https://doi.org/10.6004/jnccn.2021.0001
7. Levy-Lahad E, Friedman E. Cancer risks among BRCA1 and BRCA2 mutation carriers. *Br J Cancer*. **96,** 11–15 (2007). https://doi.org/10.1038/sj.bjc.6603535
8. McBride KA, Ballinger ML, Killick E, Kirk J, Tattersall MHN, Eeles RA, Thomas DM, Mitchell G. Li-Fraumeni syndrome: cancer risk assessment and clinical management. *Nat Rev Clin Oncol*. **11,** 260–271 (2014). https://doi.org/10.1038/nrclinonc.2014.41
9. Guan X. Cancer metastases: challenges and opportunities. *Acta Pharmaceutica Sinica B*. **5,** 402–418 (2015). https://doi.org/10.1016/j.apsb.2015.07.005
10. Eccles SA, Welch DR. Metastasis: recent discoveries and novel treatment strategies. *The Lancet*. **369,** 1742–1757 (2007). https://doi.org/10.1016/S0140-6736(07)60781-8

11. Sparrer D, Blazquez R, Keil F, Einhell S, Lüke F, Uderhardt S, Gerner C, Wendl CHR, Proescholdt M, Schulz C, Kandulski A, Haferkamp S, Schlitt HJ, Bäuerle T, Franze K, Mayr R, Rechenmacher M, Hau P, Hirsch D, Heudobler D, Evert K, Pukrop T. Primary and secondary metastatic dissemination: multiple routes to cancer-related death. *Mol Cancer*. **24,** 203 (2025). https://doi.org/10.1186/s12943-025-02389-5
12. Beckmann MW, Niederacher D, Schnürch H-G, Gusterson BA, Bender HG. Multistep carcinogenesis of breast cancer and tumour heterogeneity. *J Mol Med*. **75,** 429–439 (1997). https://doi.org/10.1007/s001090050128
13. Kittaneh M, Montero AJ, Glück S. Molecular Profiling for Breast Cancer: A Comprehensive Review. *Biomark Cancer*. **5,** BIC.S9455 (2013). https://doi.org/10.4137/BIC.S9455
14. Harbeck N, Penault-Llorca F, Cortes J, Gnant M, Houssami N, Poortmans P, Ruddy K, Tsang J, Cardoso F. Breast cancer. *Nat Rev Dis Primers*. **5,** 66 (2019). https://doi.org/10.1038/s41572-019-0111-2
15. Hammond MEH, Hayes DF, Dowsett M, Allred DC, Hagerty KL, Badve S, Fitzgibbons PL, Francis G, Goldstein NS, Hayes M, Hicks DG, Lester S, Love R, Mangu PB, McShane L, Miller K, Osborne CK, Paik S, Perlmutter J, Rhodes A, Sasano H, Schwartz JN, Sweep FCG, Taube S, Torlakovic EE, Valenstein P, Viale G, Visscher D, Wheeler T, Williams RB, Wittliff JL, Wolff AC. American Society of Clinical Oncology/College of American Pathologists Guideline Recommendations for Immunohistochemical Testing of Estrogen and Progesterone Receptors in Breast Cancer (Unabridged Version). *Arch Pathol Lab Med*. **134,** e48–e72 (2010). https://doi.org/10.5858/134.7.e48
16. Allison KH, Hammond MEH, Dowsett M, McKernin SE, Carey LA, Fitzgibbons PL, Hayes DF, Lakhani SR, Chavez-MacGregor M, Perlmutter J, Perou CM, Regan MM, Rimm DL, Symmans WF, Torlakovic EE, Varella L, Viale G, Weisberg TF, McShane LM, Wolff AC. Estrogen and Progesterone Receptor Testing in Breast Cancer: ASCO/CAP Guideline Update. *J Clin Oncol*. **38,** 1346–1366 (2020). https://doi.org/10.1200/JCO.19.02309
17. Robert NJ, Denduluri N. Patient Case Lessons: Endocrine Management of Advanced Breast Cancer. *Clin Breast Cancer*. **18,** 192–204 (2018). https://doi.org/10.1016/j.clbc.2017.05.014
18. Goss PE, Ingle JN, Pritchard KI, Robert NJ, Muss H, Gralow J, Gelmon K, Whelan T, Strasser-Weippl K, Rubin S, Sturtz K, Wolff AC, Winer E, Hudis C, Stopeck A, Beck JT, Kaur JS, Whelan K, Tu D, Parulekar WR. Extending Aromatase-Inhibitor Adjuvant

Therapy to 10 Years. *N Engl J Med*. **375,** 209–219 (2016). https://doi.org/10.1056/NEJMoa1604700

19. O'Sullivan CC. Overcoming Endocrine Resistance in Hormone-Receptor Positive Advanced Breast Cancer-The Emerging Role of CDK4/6 Inhibitors. *Int J Cancer Clin Res*. **2,** (2015). https://doi.org/10.23937/2378-3419/2/4/1029
20. Piezzo M, Chiodini P, Riemma M, Cocco S, Caputo R, Cianniello D, Di Gioia G, Di Lauro V, Rella FD, Fusco G, Iodice G, Nuzzo F, Pacilio C, Pensabene M, Laurentiis MD. Progression-Free Survival and Overall Survival of CDK 4/6 Inhibitors Plus Endocrine Therapy in Metastatic Breast Cancer: A Systematic Review and Meta-Analysis. *Int J Mol Sci*. **21,** 6400 (2020). https://doi.org/10.3390/ijms21176400
21. Johnston SRD, Harbeck N, Hegg R, Toi M, Martin M, Shao ZM, Zhang QY, Martinez Rodriguez JL, Campone M, Hamilton E, Sohn J, Guarneri V, Okada M, Boyle F, Neven P, Cortés J, Huober J, Wardley A, Tolaney SM, Cicin I, Smith IC, Frenzel M, Headley D, Wei R, San Antonio B, Hulstijn M, Cox J, O'Shaughnessy J, Rastogi P, on behalf of the monarchE Committee Members and Investigators. Abemaciclib Combined With Endocrine Therapy for the Adjuvant Treatment of HR+, HER2−, Node-Positive, High-Risk, Early Breast Cancer (monarchE). *J Clin Oncol*. **38,** 3987–3998 (2020). https://doi.org/10.1200/JCO.20.02514
22. Fusco N, Malapelle U, Fassan M, Marchiò C, Buglioni S, Zupo S, Criscitiello C, Vigneri P, Dei Tos AP, Maiorano E, Viale G. PIK3CA Mutations as a Molecular Target for Hormone Receptor-Positive, HER2-Negative Metastatic Breast Cancer. *Front Oncol*. **11,** 644737 (2021). https://doi.org/10.3389/fonc.2021.644737
23. André F, Ciruelos E, Rubovszky G, Campone M, Loibl S, Rugo HS, Iwata H, Conte P, Mayer IA, Kaufman B, Yamashita T, Lu Y-S, Inoue K, Takahashi M, Pápai Z, Longin A-S, Mills D, Wilke C, Hirawat S, Juric D. Alpelisib for *PIK3CA* -Mutated, Hormone Receptor–Positive Advanced Breast Cancer. *N Engl J Med*. **380,** 1929–1940 (2019). https://doi.org/10.1056/NEJMoa1813904
24. Baselga J, Campone M, Piccart M, Burris HA, Rugo HS, Sahmoud T, Noguchi S, Gnant M, Pritchard KI, Lebrun F, Beck JT, Ito Y, Yardley D, Deleu I, Perez A, Bachelot T, Vittori L, Xu Z, Mukhopadhyay P, Lebwohl D, Hortobagyi GN. Everolimus in Postmenopausal Hormone-Receptor–Positive Advanced Breast Cancer. *N Engl J Med*. **366,** 520–529 (2012). https://doi.org/10.1056/NEJMoa1109653

25. Osborne CK, Wakeling A, Nicholson RI. Fulvestrant: an oestrogen receptor antagonist with a novel mechanism of action. *Br J Cancer*. **90,** S2–S6 (2004). https://doi.org/10.1038/sj.bjc.6601629
26. Osborne CK, Shou J, Massarweh S, Schiff R. Crosstalk between Estrogen Receptor and Growth Factor Receptor Pathways as a Cause for Endocrine Therapy Resistance in Breast Cancer. *Clin Cancer Res*. **11,** 865s–70s (2005). https://doi.org/10.1158/1078-0432.865s.11.2
27. Neupane N, Bawek S, Gurusinghe S, Ghaffary EM, Mirmosayyeb O, Thapa S, Falkson C, O'Regan R, Dhakal A. Oral SERD, a Novel Endocrine Therapy for Estrogen Receptor-Positive Breast Cancer. *Cancers*. **16,** 619 (2024). https://doi.org/10.3390/cancers16030619
28. Bidard F-C, Kaklamani VG, Neven P, Streich G, Montero AJ, Forget F, Mouret-Reynier M-A, Sohn JH, Taylor D, Harnden KK, Khong H, Kocsis J, Dalenc F, Dillon PM, Babu S, Waters S, Deleu I, García Sáenz JA, Bria E, Cazzaniga M, Lu J, Aftimos P, Cortés J, Liu S, Tonini G, Laurent D, Habboubi N, Conlan MG, Bardia A. Elacestrant (oral selective estrogen receptor degrader) Versus Standard Endocrine Therapy for Estrogen Receptor–Positive, Human Epidermal Growth Factor Receptor 2–Negative Advanced Breast Cancer: Results From the Randomized Phase III EMERALD Trial. *J Clin Oncol*. **40,** 3246–3256 (2022). https://doi.org/10.1200/JCO.22.00338
29. Varella L, Cristofanilli M. Evaluating Elacestrant in the Management of ER-Positive, HER2-Negative Advanced Breast Cancer: Evidence to Date. *Onco Targets Ther*. **Volume 16,** 189–196 (2023). https://doi.org/10.2147/OTT.S400563
30. Molehin D, Filleur S, Pruitt K. Regulation of aromatase expression: Potential therapeutic insight into breast cancer treatment. *Mol Cell Endocrinol*. **531,** 111321 (2021). https://doi.org/10.1016/j.mce.2021.111321
31. Reed MJ, Purohit A, Woo LWL, Newman SP, Potter BVL. Steroid Sulfatase: Molecular Biology, Regulation, and Inhibition. *Endocr Rev*. **26,** 171–202 (2005). https://doi.org/10.1210/er.2004-0003
32. Azzouni F, Godoy A, Li Y, Mohler J. The 5 Alpha-Reductase Isozyme Family: A Review of Basic Biology and Their Role in Human Diseases. *Adv Urol*. **2012,** 1–18 (2012). https://doi.org/10.1155/2012/530121
33. Chapman K, Holmes M, Seckl J. 11β-Hydroxysteroid Dehydrogenases: Intracellular Gate-Keepers of Tissue Glucocorticoid Action. *Physiol Rev*. **93,** 1139–1206 (2013). https://doi.org/10.1152/physrev.00020.2012

34. Jin P, Duan X, Huang Z, Dong Y, Zhu J, Guo H, Tian H, Zou C-G, Xie K. Nuclear receptors in health and disease: signaling pathways, biological functions and pharmaceutical interventions. *Sig Transduct Target Ther*. **10,** 228 (2025). https://doi.org/10.1038/s41392-025-02270-3
35. Treviño LS, Gorelick DA. The Interface of Nuclear and Membrane Steroid Signaling. *Endocrinology*. **162,** bqab107 (2021). https://doi.org/10.1210/endocr/bqab107
36. Tantawy MA, Nafie MS, Elmegeed GA, Ali IAI. Auspicious role of the steroidal heterocyclic derivatives as a platform for anti-cancer drugs. *Bioorg Chem*. **73,** 128–146 (2017). https://doi.org/10.1016/j.bioorg.2017.06.006
37. Michael P, Roversi G, Brown K, Sharifi N. Adrenal Steroids and Resistance to Hormonal Blockade of Prostate and Breast Cancer. *Endocrinology*. **164,** bqac218 (2023). https://doi.org/10.1210/endocr/bqac218
38. Huggins C, Hodges CV. Studies on prostatic cancer. I. The effect of castration, of estrogen and androgen injection on serum phosphatases in metastatic carcinoma of the prostate. *CA Cancer J Clin*. **22,** 232–240 (1972). https://doi.org/10.3322/canjclin.22.4.232
39. McRobb FM, Kufareva I, Abagyan R. *In Silico* Identification and Pharmacological Evaluation of Novel Endocrine Disrupting Chemicals That Act via the Ligand-Binding Domain of the Estrogen Receptor α. *Toxicol Sci*. **141,** 188–197 (2014). https://doi.org/10.1093/toxsci/kfu114
40. Shimmin BA, Haines LG, Shaw IC. *In silico* studies on the molecular interactions of steroid hormones and steroid hormone mimicking drugs in the androgen receptor binding cleft – Implications for prostate cancer treatment. *Steroids*. **208,** 109456 (2024). https://doi.org/10.1016/j.steroids.2024.109456
41. Heemers HV, Tindall DJ. Androgen Receptor (AR) Coregulators: A Diversity of Functions Converging on and Regulating the AR Transcriptional Complex. *Endocr Rev*. **28,** 778–808 (2007). https://doi.org/10.1210/er.2007-0019
42. Razandi M, Pedram A, Merchenthaler I, Greene GL, Levin ER. Plasma Membrane Estrogen Receptors Exist and Functions as Dimers. *Mol Endocrinol*. **18,** 2854–2865 (2004). https://doi.org/10.1210/me.2004-0115
43. Nye AC, Rajendran RR, Stenoien DL, Mancini MA, Katzenellenbogen BS, Belmont AS. Alteration of Large-Scale Chromatin Structure by Estrogen Receptor. *Mol Cell Biol*. **22,** 3437–3449 (2002). https://doi.org/10.1128/MCB.22.10.3437-3449.2002
44. Hebbar PB, Archer TK. Chromatin remodeling by nuclear receptors. *Chromosoma*. **111,** 495–504 (2003). https://doi.org/10.1007/s00412-003-0232-x

45. Khan SH, Braet SM, Koehler SJ, Elacqua E, Anand GS, Okafor CD. Ligand-induced shifts in conformational ensembles that describe transcriptional activation. *eLife*. **11,** e80140 (2022). https://doi.org/10.7554/eLife.80140
46. Chimento A, De Luca A, Avena P, De Amicis F, Casaburi I, Sirianni R, Pezzi V. Estrogen Receptors-Mediated Apoptosis in Hormone-Dependent Cancers. *Int J Mol Sci*. **23,** 1242 (2022). https://doi.org/10.3390/ijms23031242
47. Kaufmann M, Bajetta E, Dirix LY, Fein LE, Jones SE, Zilembo N, Dugardyn J-L, Nasurdi C, Mennel RG, Cervek J, Fowst C, Polli A, Di Salle E, Arkhipov A, Piscitelli G, Miller LL, Massimini G, for the Exemestane Study Group. Exemestane Is Superior to Megestrol Acetate After Tamoxifen Failure in Postmenopausal Women With Advanced Breast Cancer: Results of a Phase III Randomized Double-Blind Trial. *J Clin Oncol*. **18,** 1399–1411 (2000). https://doi.org/10.1200/JCO.2000.18.7.1399
48. Hinkel A, Berges RR, Pannek J, Schulze H, Senge Th. Cyproterone Acetate in theTreatment of Advanced ProstaticCancer: Retrospective Analysis ofLiver Toxicity in the Long-TermFollow-Up of 89 Patients. *Eur Urol*. **30,** 464–470 (1996). https://doi.org/10.1159/000474216
49. Stenkvist B, Bengtsson E, Eriksson O, Holmquist J, Nordin B, Westman-Naeser S, Eklund G. Cardiac glycosides and breast cancer. *Lancet*. **313,** 563 (1979). https://doi.org/10.1016/S0140-6736(79)90996-6
50. Geng X, Wang F, Tian D, Huang L, Streator E, Zhu J, Kurihara H, He R, Yao X, Zhang Y, Tang J. Cardiac glycosides inhibit cancer through Na/K-ATPase-dependent cell death induction. *Biochem Pharmacol*. **182,** 114226 (2020). https://doi.org/10.1016/j.bcp.2020.114226
51. Nik Nabil WN, Dai R, Liu M, Xi Z, Xu H. Repurposing cardiac glycosides for anticancer treatment: a review of clinical studies. *Drug Discov Today*. **29,** 104129 (2024). https://doi.org/10.1016/j.drudis.2024.104129
52. Lottering M-L, Haag M, Seegers JC. Effects of 17β-Estradiol Metabolites on Cell Cycle Events in MCF-7 Cells. *Cancer Res*. **52,** 5926–5932 (1992).
53. LaVallee TM, Zhan XH, Herbstritt CJ, Kough EC, Green SJ, Pribluda VS. 2-Methoxyestradiol inhibits proliferation and induces apoptosis independently of estrogen receptors alpha and beta. *Cancer Res*. **62,** 3691–3697 (2002).
54. Mendoza Lara DF, Hernández-Caballero ME, Terán JL, Ramírez JS, Carrasco-Carballo A. Anticancer Activities of Natural and Synthetic Steroids: A Review. *ACS Omega*. **10,** 7493–7509 (2025). https://doi.org/10.1021/acsomega.4c08577

55. Kovács F, Huliák I, Árva H, Kocsis M, Kiricsi M, Frank É. Aromatic scaffold-integrated hybrids of estradiol and benzoxazol-2-ones: synthesis and *in vitro* anticancer activity of *N* -substituted regioisomeric pairs. *RSC Adv*. **15,** 23954–23965 (2025). https://doi.org/10.1039/D5RA01977J
56. Ke S, Shi L, Zhang Z, Yang Z. Steroidal[17,16-*d*]pyrimidines derived from dehydroepiandrosterone: A convenient synthesis, antiproliferation activity, structure-activity relationships, and role of heterocyclic moiety. *Sci Rep*. **7,** 44439 (2017). https://doi.org/10.1038/srep44439
57. Minorics R, Zupko I. Steroidal Anticancer Agents: An Overview of Estradiol-related Compounds. *Anticancer Agents Med Chem*. **18,** 652–666 (2018). https://doi.org/10.2174/1871520617666171114111721
58. Ibrahim-Ouali M, Santelli M. Recent advances in thiasteroids chemistry. *Steroids*. **71,** 1025–1044 (2006). https://doi.org/10.1016/j.steroids.2006.09.006
59. Frank É, Schneider G. Synthesis of sex hormone-derived modified steroids possessing antiproliferative activity. *J Steroid Biochem Mol Biol*. **137,** 301–315 (2013). https://doi.org/10.1016/j.jsbmb.2013.02.018
60. Wölfling J, Mernyák E, Sebők M, Schneider G. Synthesis of Some Steroidal Oxazolines. *Collect Czech Chem Commun*. **66,** 1831–1840 (2001). https://doi.org/10.1135/cccc20011831
61. Hajnal A, Wölfling J, Schneider Gy. Novel Preparation of Dihydrooxazines Condensed to Ring D of the Estrane Skeleton. *Synlett*. **2002,** 1077–1080 (2002). https://doi.org/10.1055/s-2002-32590
62. Schönecker B, Lange C, Kötteritzsch M, Günther W, Weston J, Anders E, Görls H. Conformational Design for 13α-Steroids. *J Org Chem*. **65,** 5487–5497 (2000). https://doi.org/10.1021/jo000108x
63. Ayan D, Roy J, Maltais R, Poirier D. Impact of estradiol structural modifications (18-methyl and/or 17-hydroxy inversion of configuration) on the *in vitro* and *in vivo* estrogenic activity. *J Steroid Biochem Mol Biol*. **127,** 324–330 (2011). https://doi.org/10.1016/j.jsbmb.2011.07.009
64. Demkowicz S, Rachon J, Daśko M, Kozak W. Selected organophosphorus compounds with biological activity. Applications in medicine. *RSC Adv*. **6,** 7101–7112 (2016). https://doi.org/10.1039/C5RA25446A
65. Kiss A, Jójárt R, Mernyák E, Bartha S, Minorics R, Zupkó I, Schneider G. Novel preparation of substituted oxazolines condensed to D-ring of estrane skeleton and

characterization of their antiproliferative properties. *Steroids*. **176,** 108911 (2021). https://doi.org/10.1016/j.steroids.2021.108911

66. Mernyák E, Bartha S, Kóczán L, Jójárt R, Resch V, Paragi G, Vágvölgyi M, Hunyadi A, Bruszel B, Zupkó I, Minorics R. Microwave-assisted Phospha-Michael addition reactions in the 13α-oestrone series and *in vitro* antiproliferative properties. *J Enzyme Inhib Med Chem*. **36,** 1931–1937 (2021). https://doi.org/10.1080/14756366.2021.1963241
67. Wakeling AE, Bowler J. ICI 182,780, a new antioestrogen with clinical potential. *J Steroid Biochem Mol Biol*. **43,** 173–177 (1992). https://doi.org/10.1016/0960-0760(92)90204-V
68. Vermes I, Haanen C, Reutelingsperger C. Flow cytometry of apoptotic cell death. *J Immunol Methods*. **243,** 167–190 (2000). https://doi.org/10.1016/S0022-1759(00)00233-7
69. Dolfi SC, Jäger AV, Medina DJ, Haffty BG, Yang J-M, Hirshfield KM. Fulvestrant treatment alters MDM2 protein turnover and sensitivity of human breast carcinoma cells to chemotherapeutic drugs. *Cancer Lett*. **350,** 52–60 (2014). https://doi.org/10.1016/j.canlet.2014.04.009
70. Behrens J, Kameritsch P, Wallner S, Pohl U, Pogoda K. The carboxyl tail of Cx43 augments p38 mediated cell migration in a gap junction-independent manner. *Eur J Cell Biol*. **89,** 828–838 (2010). https://doi.org/10.1016/j.ejcb.2010.06.003
71. Saatci O, Huynh-Dam K-T, Sahin O. Endocrine resistance in breast cancer: from molecular mechanisms to therapeutic strategies. *J Mol Med*. **99,** 1691–1710 (2021). https://doi.org/10.1007/s00109-021-02136-5
72. Szostakowska M, Trębińska-Stryjewska A, Grzybowska EA, Fabisiewicz A. Resistance to endocrine therapy in breast cancer: molecular mechanisms and future goals. *Breast Cancer Res Treat*. **173,** 489–497 (2019). https://doi.org/10.1007/s10549-018-5023-4
73. Hanker AB, Sudhan DR, Arteaga CL. Overcoming Endocrine Resistance in Breast Cancer. *Cancer Cell*. **37,** 496–513 (2020). https://doi.org/10.1016/j.ccell.2020.03.009
74. Raheem F, Karikalan SA, Batalini F, El Masry A, Mina L. Metastatic ER+ Breast Cancer: Mechanisms of Resistance and Future Therapeutic Approaches. *Int J Mol Sci*. **24,** 16198 (2023). https://doi.org/10.3390/ijms242216198
75. Chavez KJ, Garimella SV, Lipkowitz S. Triple negative breast cancer cell lines: One tool in the search for better treatment of triple negative breast cancer. *Breast Dis*. **32,** 35–48 (2011). https://doi.org/10.3233/BD-2010-0307
76. Björnström L, Sjöberg M. Mechanisms of Estrogen Receptor Signaling: Convergence of Genomic and Nongenomic Actions on Target Genes. *Mol Endocrinol*. **19,** 833–842 (2005). https://doi.org/10.1210/me.2004-0486

77. Wilson VS. Development and Characterization of a Cell Line That Stably Expresses an Estrogen-Responsive Luciferase Reporter for the Detection of Estrogen Receptor Agonist and Antagonists. *Toxicol Sci*. **81,** 69–77 (2004). https://doi.org/10.1093/toxsci/kfh180
78. OECD. *Test No. 440: Uterotrophic Bioassay in Rodents: A short-term screening test for oestrogenic properties*. (OECD, 2007). doi:10.1787/9789264067417-en https://doi.org/10.1787/9789264067417-en
79. Bartha S, Germán P, Bózsity N, Puskás LG, Börzsei R, Hetényi C, Zupkó I, Mernyák E, Minorics R. Biological and computer-aided evaluation of 3-methoxy-13α-estrone-16α-diphenylphosphine oxide as a new antiestrogenic agent. *Sci Rep*. **15,** 44295 (2025). https://doi.org/10.1038/s41598-025-27905-x
80. Brzozowski AM, Pike ACW, Dauter Z, Hubbard RE, Bonn T, Engström O, Öhman L, Greene GL, Gustafsson J-Å, Carlquist M. Molecular basis of agonism and antagonism in the oestrogen receptor. *Nature*. **389,** 753–758 (1997). https://doi.org/10.1038/39645
81. Arao Y, Korach KS. The physiological role of estrogen receptor functional domains. *Essays Biochem*. **65,** 867–875 (2021). https://doi.org/10.1042/EBC20200167
82. Nettles KW, Greene GL. Ligand Control of Coregulator Cecruitment to Nuclear Receptors. *Annu Rev Physiol*. **67,** 309–333 (2005). https://doi.org/10.1146/annurev.physiol.66.032802.154710
83. Gajadeera N, Hanson RN. Review of fluorescent steroidal ligands for the estrogen receptor 1995–2018. *Steroids*. **144,** 30–46 (2019). https://doi.org/10.1016/j.steroids.2019.02.002
84. Delfosse V, Grimaldi M, Pons J-L, Boulahtouf A, Le Maire A, Cavailles V, Labesse G, Bourguet W, Balaguer P. Structural and mechanistic insights into bisphenols action provide guidelines for risk assessment and discovery of bisphenol A substitutes. *Proc Natl Acad Sci U S A*. **109,** 14930–14935 (2012). https://doi.org/10.1073/pnas.1203574109
85. Prall OwenWJ, Sarcevic B, Musgrove EA, Watts ColinKW, Sutherland RL. Estrogen-induced Activation of Cdk4 and Cdk2 during G_1-S Phase Progression Is Accompanied by Increased Cyclin D1 Expression and Decreased Cyclin-dependent Kinase Inhibitor Association with Cyclin E-Cdk2. *J Biol Chem*. **272,** 10882–10894 (1997). https://doi.org/10.1074/jbc.272.16.10882
86. Swetzig WM, Wang J, Das GM. Estrogen receptor alpha (ERα/ESR1) mediates the p53-independent overexpression of MDM4/MDMX and MDM2 in human breast cancer. *Oncotarget*. **7,** 16049–16069 (2016). https://doi.org/10.18632/oncotarget.7533

87. Martin K, Trouche D, Hagemeier C, Sørensen TS, La Thangue NB, Kouzarides T. Stimulation of E2F1/DP1 transcriptional activity by MDM2 oncoprotein. *Nature*. **375,** 691–694 (1995). https://doi.org/10.1038/375691a0
88. Caldon CE, Sergio CM, Schütte J, Boersma MN, Sutherland RL, Carroll JS, Musgrove EA. Estrogen Regulation of Cyclin E2 Requires Cyclin D1 but Not c-Myc. *Mol Cell Biol*. **29,** 4623–4639 (2009). https://doi.org/10.1128/MCB.00269-09
89. Akiyama T, Ohuchi T, Sumida S, Matsumoto K, Toyoshima K. Phosphorylation of the retinoblastoma protein by cdk2. *Proc Natl Acad Sci U S A*. **89,** 7900–7904 (1992). https://doi.org/10.1073/pnas.89.17.7900
90. Engeland K. Cell cycle regulation: p53-p21-RB signaling. *Cell Death Differ*. **29,** 946–960 (2022). https://doi.org/10.1038/s41418-022-00988-z
91. Giretti MS, Fu X-D, De Rosa G, Sarotto I, Baldacci C, Garibaldi S, Mannella P, Biglia N, Sismondi P, Genazzani AR, Simoncini T. Extra-Nuclear Signalling of Estrogen Receptor to Breast Cancer Cytoskeletal Remodelling, Migration and Invasion. *PLoS ONE*. **3,** e2238 (2008). https://doi.org/10.1371/journal.pone.0002238
92. Sanchez AM, Flamini MI, Baldacci C, Goglia L, Genazzani AR, Simoncini T. Estrogen Receptor-α Promotes Breast Cancer Cell Motility and Invasion via Focal Adhesion Kinase and N-WASP. *Mol Endocrinol*. **24,** 2114–2125 (2010). https://doi.org/10.1210/me.2010-0252
93. Rajah TT, Rambo DJ, Dmytryk JJ, Pento JT. Influence of Antiestrogens on NIH-3T3-Fibroblast-Induced Motility of Breast Cancer Cells. *Chemotherapy*. **47,** 56–69 (2001). https://doi.org/10.1159/000048502
94. Egloff AM, Rothstein ME, Seethala R, Siegfried JM, Grandis JR, Stabile LP. Cross-Talk between Estrogen Receptor and Epidermal Growth Factor Receptor in Head and Neck Squamous Cell Carcinoma. *Clin Cancer Res*. **15,** 6529–6540 (2009). https://doi.org/10.1158/1078-0432.CCR-09-0862
95. Svoronos N, Perales-Puchalt A, Allegrezza MJ, Rutkowski MR, Payne KK, Tesone AJ, Nguyen JM, Curiel TJ, Cadungog MG, Singhal S, Eruslanov EB, Zhang P, Tchou J, Zhang R, Conejo-Garcia JR. Tumor Cell–Independent Estrogen Signaling Drives Disease Progression through Mobilization of Myeloid-Derived Suppressor Cells. *Cancer Discov*. **7,** 72–85 (2017). https://doi.org/10.1158/2159-8290.CD-16-0502
96. Kajihara N, Ge Y, Seino K. Blocking of oestrogen signals improves anti-tumour effect regardless of oestrogen receptor alpha expression in cancer cells. *Br J Cancer*. **129,** 935–946 (2023). https://doi.org/10.1038/s41416-023-02381-0

9. Acknowledgements

First, I would like to express my sincerest gratitude to my supervisor, Dr. Renáta Minorics, whose constant support, guidance, enthusiasm, professional insight, and friendly attitude throughout all these years of collaboration were essential in bringing this PhD thesis to completion.

I am also deeply grateful to Professor Dr. István Zupkó, Head of the Institute of Pharmacodynamics and Biopharmacy and former Dean of the Faculty of Pharmacy. I thank him for accepting me into the PhD program, for sharing his extensive knowledge in the field, for his guidance, and support throughout my work.

I would further like to acknowledge all collaborating partners for their valuable contributions to the design and synthesis of the tested compounds, as well as for conducting essential experiments related to my research. In particular, I wish to thank Dr. Erzsébet Mernyák, Dr. Csaba Hetényi, Dr. László G. Puskás, and the late Professor Dr. Gyula Schneider.

My sincere thanks also go to all current and former colleagues at the Institute of Pharmacodynamics, whose support and collegiality greatly contributed to making my professional life easier and more enjoyable. Special thanks go to Dr. Noémi Bózsity-Faragó and Péter Germán for their valuable contribution to the experimental work.

Finally, I would like to express my deepest gratitude to my parents, Nóra Harsányi and Dr. Imre Bartha, to my partner in life, Judit Papp, and to my friends, whose unwavering support and encouragement toward my goals provided the greatest motivation for completing my PhD studies. I could not have done it without you.